



## Towards artificial photosynthesis: Sustainable hydrogen utilization for photocatalytic reduction of CO<sub>2</sub> to high-value renewable fuels



Van-Huy Nguyen<sup>a,b,\*</sup>, Ba-Son Nguyen<sup>c</sup>, Zhong Jin<sup>d</sup>, Mohammadreza Shokouhimehr<sup>e</sup>,  
Ho Won Jang<sup>e</sup>, Chechia Hu<sup>f</sup>, Pardeep Singh<sup>g</sup>, Pankaj Raizada<sup>g</sup>, Wanxi Peng<sup>h</sup>, Su Shiung Lam<sup>i</sup>,  
Changlei Xia<sup>j,k</sup>, Chinh Chien Nguyen<sup>l,m,\*</sup>, Soo Young Kim<sup>n,\*</sup>, Quyet Van Le<sup>l,\*</sup>

<sup>a</sup> Department for Management of Science and Technology Development, Ton Duc Thang University, Ho Chi Minh City, Vietnam

<sup>b</sup> Faculty of Applied Sciences, Ton Duc Thang University, Ho Chi Minh City, Vietnam

<sup>c</sup> Key Laboratory of Advanced Materials for Energy and Environmental Applications, Lac Hong University, Bien Hoa, Vietnam

<sup>d</sup> Jiangsu Key Laboratory of Advanced Organic Materials, Key Laboratory of Mesoscopic Chemistry of MOE, School of Chemistry and Chemical Engineering, Nanjing University, Nanjing, Jiangsu 210023, China

<sup>e</sup> Department of Materials Science and Engineering, Research Institute of Advanced Materials, Seoul National University, Seoul 08826, Republic of Korea

<sup>f</sup> Department of Chemical Engineering, R&D Center for Membrane Technology and Research Center for Circular Economy, Chung Yuan Christian University, Chungli Dist., Taoyuan City 32023, Taiwan

<sup>g</sup> School of Chemistry, Faculty of Basic Sciences, Shoolini University, Solan Himachal Pradesh 173212, India

<sup>h</sup> Henan Province Engineering Research Center for Biomass Value-added Products, School of Forestry, Henan Agricultural University, Zhengzhou, 450002, China

<sup>i</sup> Pyrolysis Technology Research Group, Institute of Tropical Aquaculture and Fisheries (Akuatrop) & Institute of Tropical Biodiversity and Sustainable Development (Bio-D Tropika), Universiti Malaysia Terengganu, 21030 Kuala Terengganu, Terengganu, Malaysia

<sup>j</sup> Co-Innovation Center of Efficient Processing and Utilization of Forestry Resources, College of Materials Science and Engineering, Nanjing Forestry University, Nanjing, Jiangsu 210037, China

<sup>k</sup> Anhui Juke Graphene Technology Co., Ltd. Bozhou, 233600, China

<sup>l</sup> Institute of Research and Development, Duy Tan University, Da Nang 550000, Vietnam

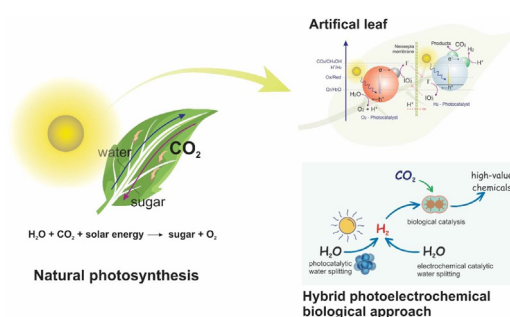
<sup>m</sup> Faculty of Environmental and Chemical Engineering, Duy Tan University, Da Nang 550000, Vietnam

<sup>n</sup> Department of Materials Science and Engineering, Korea University, 145, Anam-ro Seongbuk-gu, Seoul 02841, Republic of Korea

### HIGHLIGHTS

- Artificial photosynthesis for reduction of CO<sub>2</sub> to renewable fuels was reviewed.
- Various photocatalysts and reaction parameters for photoreduction of CO<sub>2</sub> were summarized and discussed.
- The CO<sub>2</sub> photoreduction to mimic natural photosynthesis was proposed and verified successfully.

### GRAPHICAL ABSTRACT



### ARTICLE INFO

#### Keywords:

Artificial synthesis  
Photocatalysts

### ABSTRACT

Converting solar energy into fuel via photo-assisted water splitting to generate H<sub>2</sub> or drive CO<sub>2</sub> photoreduction is an attractive scientific and technological goal to address the increasing global demand for energy and to reduce the impact of energy production on climate change. Solar-driven hydrogenation of CO<sub>2</sub> into value-added

\* Corresponding authors at: Ton Duc Thang University, Ho Chi Minh City, Vietnam (V.-H. Nguyen). Duy Tan University, Da Nang 550000, Vietnam (C.C. Nguyen, Q.V. Le). Korea University, Seoul 02841, Republic of Korea (S.Y. Kim).

E-mail addresses: [nguyenvanhuy@tdtu.edu.vn](mailto:nguyenvanhuy@tdtu.edu.vn) (V.-H. Nguyen), [nguyenchinhchien@duytan.edu.vn](mailto:nguyenchinhchien@duytan.edu.vn) (C.C. Nguyen), [sooyoungkim@korea.ac.kr](mailto:sooyoungkim@korea.ac.kr) (S.Y. Kim), [levanquyet@dtu.edu.vn](mailto:levanquyet@dtu.edu.vn) (Q.V. Le).

<https://doi.org/10.1016/j.cej.2020.126184>

Received 10 April 2020; Received in revised form 4 June 2020; Accepted 3 July 2020

Available online 08 July 2020

1385-8947/ © 2020 Elsevier B.V. All rights reserved.

chemical products is one of the most promising strategies for reducing CO<sub>2</sub> and is anticipated to be a sustainable energy source shortly. In this study, we focus on the utilization of different sustainable H<sub>2</sub> sources for the photoreduction of CO<sub>2</sub> to value-added organic products. Various photocatalysts, photoreactor configurations, and reaction parameters for the photoreduction of CO<sub>2</sub> are discussed. For future research endeavors, a general approach for the photoreduction of CO<sub>2</sub> to mimic natural photosynthesis, in which the H<sub>2</sub> source is provided directly during the photocatalytic water splitting, is proposed and verified to generate value-added organic products successfully.

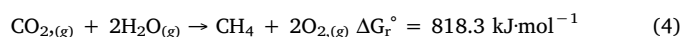
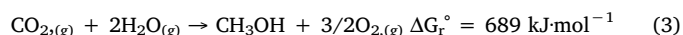
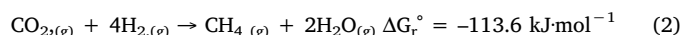
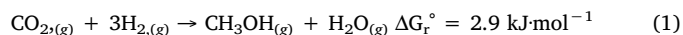
## 1. Introduction

With the significant increase in the levels of greenhouse gases, such as carbon dioxide (CO<sub>2</sub>), in the atmosphere, considerable effort has been directed toward the development of methods for efficient CO<sub>2</sub> utilization. There is a wide range of literature on this topic [1,2]. Practically, CO<sub>2</sub> is a relatively inert and stable molecule ( $\Delta G^\circ = -400 \text{ kJ}\cdot\text{mol}^{-1}$ ) that requires a catalyst and input energy to be activated and converted into another chemical form [3–7]. CO<sub>2</sub> has attracted considerable attention as a C building block for generating high-value renewable solar fuels, and photocatalytic reduction (photoreduction) is a promising approach for storing solar energy and chemically reducing CO<sub>2</sub>. In the recent few decades, many studies have been systematically examined and published on this subject [8–28]. However, the current conversion rate is unsatisfactory, emphasizing the need for further studies [1]. Many reducing substances can function as both H<sub>2</sub> sources and hole scavengers (also referred to as “electron donors”) for promoting CO<sub>2</sub> reduction (e.g., water (H<sub>2</sub>O), H<sub>2</sub>, methane (CH<sub>4</sub>), and alcohols such as methanol (CH<sub>3</sub>OH) and ethanol (C<sub>2</sub>H<sub>5</sub>OH)), leading to different high-value chemical products [29]. According to previous studies, C-free reductants, such as H<sub>2</sub>O and H<sub>2</sub>, drive the generation of C<sub>1</sub> products, whereas C-containing reductants, such as CH<sub>4</sub>, CH<sub>3</sub>OH, and C<sub>2</sub>H<sub>5</sub>OH, yield C<sub>2</sub> and C<sub>3</sub> products [30]. The H<sub>2</sub> source can be simply obtained via electrocatalytic or photocatalytic water splitting [31–43]. To focus on the eco-friendly, renewable production of high-value chemicals from CO<sub>2</sub>, C-free reductants, including H<sub>2</sub>O and H<sub>2</sub>, are investigated in this review.

The photoreduction of CO<sub>2</sub> with H<sub>2</sub>O is of particular interest. Very early, Inoue et al. presented a potential approach for reducing CO<sub>2</sub> to organic compounds such as formic acid, formaldehyde, methyl alcohol, and methane using H<sub>2</sub>O [44]. Subsequently, many studies were conducted on heterogeneous photocatalytic systems for elucidating the fundamental mechanisms, and inorganic semiconductor photocatalysts were engineered to capture light and accelerate the chemical reactions productively. Homogeneous photocatalytic systems have been used for the latter; however, molecular photosensitizers (dyes) could not provide a more realistic and robust concept [45].

According to the theoretical changes of the Gibbs free energy ( $\Delta G_r^\circ$ )

for CO<sub>2</sub> reduction to generate hydrocarbons, such as CH<sub>3</sub>OH and CH<sub>4</sub>, the hydrogenation of CO<sub>2</sub> by H<sub>2</sub> to produce hydrocarbons (Eqs. (1) and (2)) is more feasible than the reduction of CO<sub>2</sub> by H<sub>2</sub>O (Eqs. (3) and (4)) from a thermodynamic viewpoint [30].



To learn this theory, photocatalytic reduction (photoreduction) of CO<sub>2</sub> by H<sub>2</sub> gas as a sacrificial electron donor under light irradiation has been proposed. This promising approach not only spontaneously hydrogenates CO<sub>2</sub> emission but also simultaneously transforms CO<sub>2</sub> into renewable organic compounds, such as methanol and hydrocarbons. Thampi et al. first reported photo-hydrogenation of CO<sub>2</sub> to CH<sub>4</sub> (49  $\mu\text{mol}\cdot\text{g}_{\text{cat}}^{-1}\cdot\text{h}^{-1}$ ) by H<sub>2</sub> over Ru/RuOx/TiO<sub>2</sub> using a solar simulator (319 K; 80  $\text{mW}\cdot\text{cm}^{-2}$ ) [46]. In addition to CH<sub>4</sub> [47–50], other products, such as carbon monoxide (CO) [47–62], ethane (C<sub>2</sub>H<sub>6</sub>) [47,50,54], and CH<sub>3</sub>OH [60,61,63–65] have been obtained, depending on the photocatalytic materials and experimental conditions.

Artificial photosynthesis—another promising approach that was recently proposed—combines solar-driven water splitting and CO<sub>2</sub> reduction and is based on natural photosynthesis, as illustrated in Fig. 1. In this method, active H, which is directly produced from photocatalytic water splitting, is continuously used for the photoreduction of CO<sub>2</sub> to produce solar fuel in the same photocatalytic systems. Guan et al. first proposed mimicking the natural photosynthesis process by using hybrid photocatalysts [66]. In this regard, the active H, which was directly supplied via the sustainable photocatalytic water splitting, was continuously used for the photo-hydrogenation of CO<sub>2</sub> over hybrid photocatalysts to produce organic compounds.

Up to date, several review articles are covering structural engineering semiconductors, particular materials, their structure and applications for photoreduction of CO<sub>2</sub>, such as sunlight-driven photocatalysts [13], crystal phase engineering on photocatalysts [67], metal-free-based materials [68], ultrathin structured photocatalysts

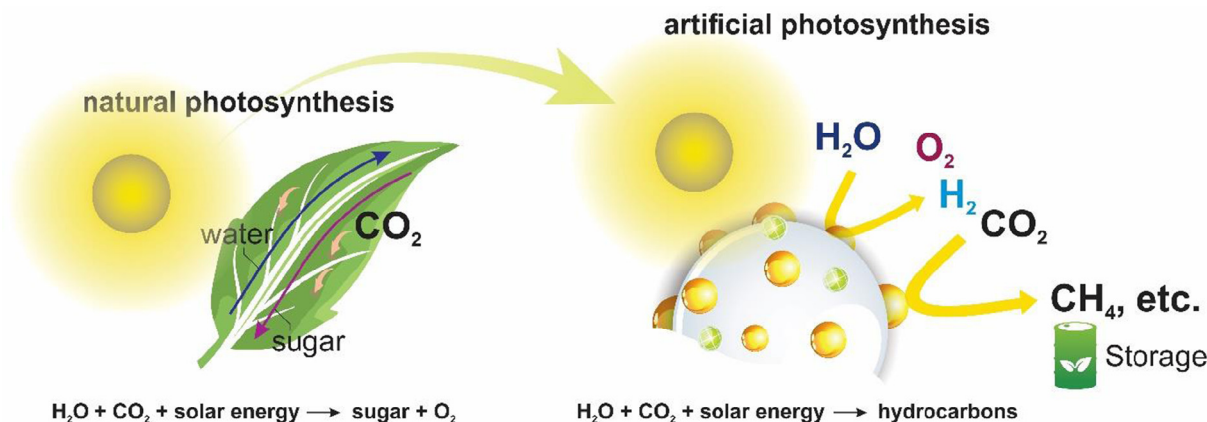


Fig. 1. Conversion of solar energy: natural leaf and mimicking photosynthesis in artificial systems via photocatalysis.

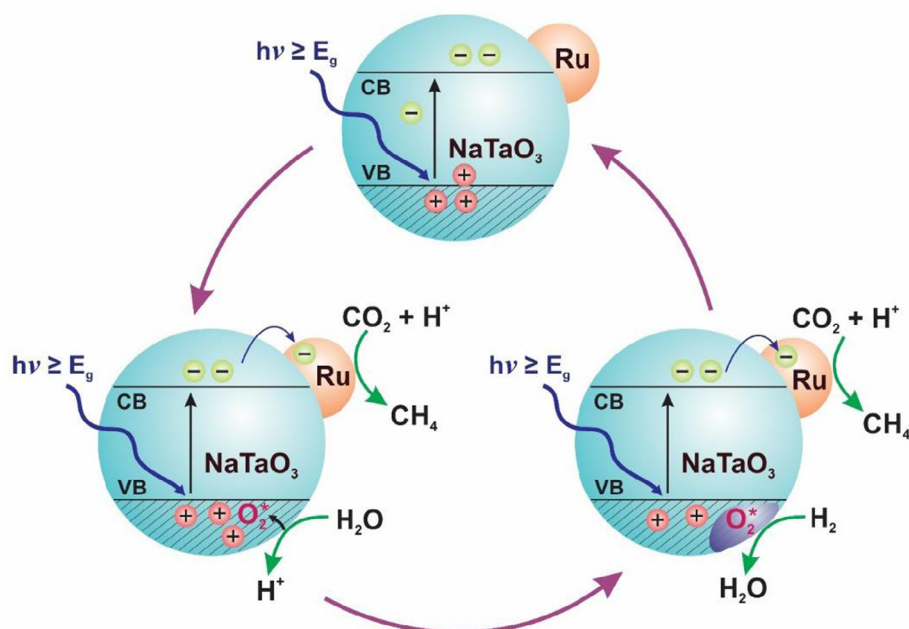


Fig. 2. Photoreduction of  $\text{CO}_2$  over Ru/NaTaO<sub>3</sub> in the presence of H<sub>2</sub>O and H<sub>2</sub>. Reproduced with permission from Ref. [49].

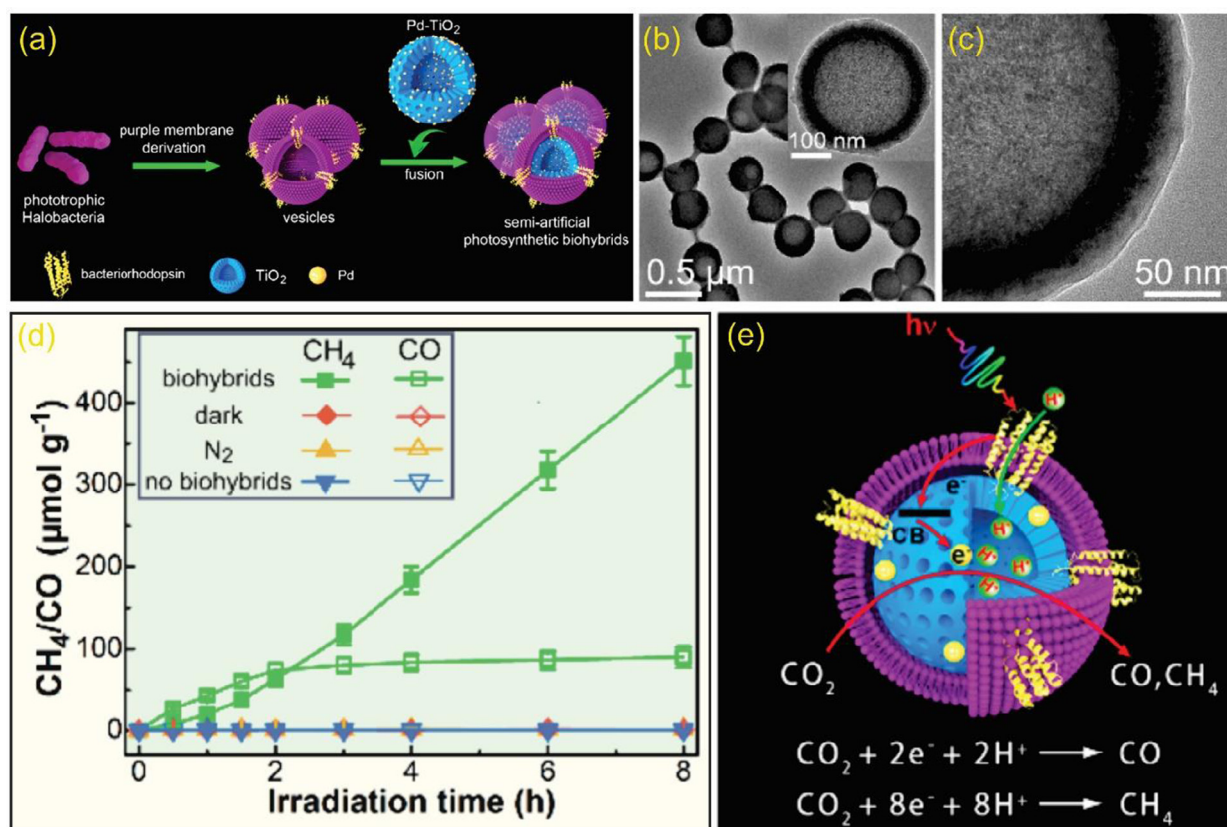


Fig. 3. (a) Preparation of Halobacterium purple membrane-derived vesicles with Pd-deposited hollow porous TiO<sub>2</sub> NPs (Pd-HTNPs@PMVs). (b, c) Magnified transmission electron microscopy (TEM) image showing the edge of a single Pd-HTNPs@PMVs. (d) Photocatalytic CH<sub>4</sub> and CO formation over the biohybrids (Pd-HTNPs@PMVs) under different conditions. (e) Proposed process of photoreduction of CO<sub>2</sub> by Pd-HTNPs@PMVs. Reproduced with permission from Ref. [75]. (For interpretation of the references to colour in this figure legend, the reader is referred to the web version of this article.)

[69], cocatalysts [70], Bismuth-based photocatalysts [71]. Additionally, other reviews concentrate on tuning product selectivity [72], surface strategies for particulate photocatalysts [73], general aspects of light-driven C1 chemistry, including solar Fischer-Tropsch synthesis,

the water-gas-shift reaction, CO<sub>2</sub> hydrogenation, as well as methane and methanol conversion reactions [74]. Since the overall knowledge of chemical engineering for transforming the CO<sub>2</sub> into value-added products using energy-efficient processes has significantly increased in the

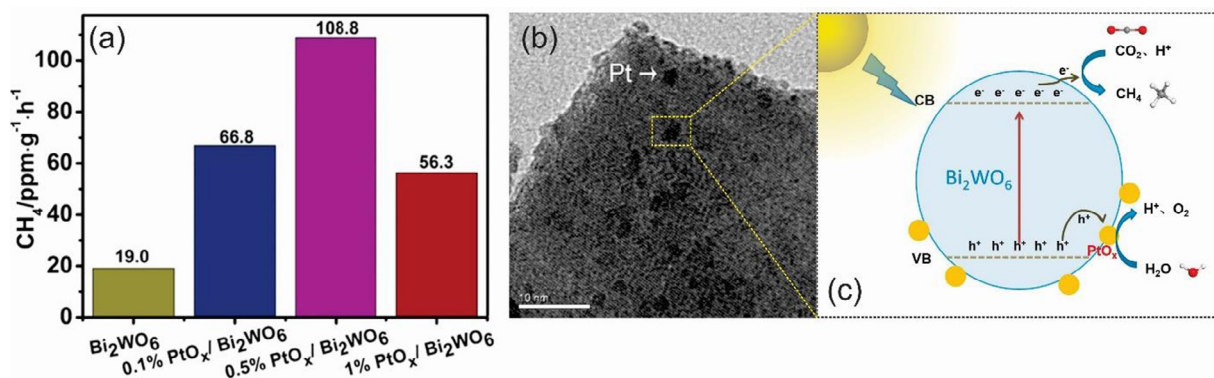


Fig. 4. (a) CH<sub>4</sub> production rate with respect to the loading amount (wt.%) of PtO<sub>x</sub>. (b) TEM image of 0.5%PtO<sub>x</sub>/Bi<sub>2</sub>WO<sub>6</sub>. (c) Proposed mechanism over PtO<sub>x</sub>/Bi<sub>2</sub>WO<sub>6</sub>. Reproduced with permission from Ref. [77].

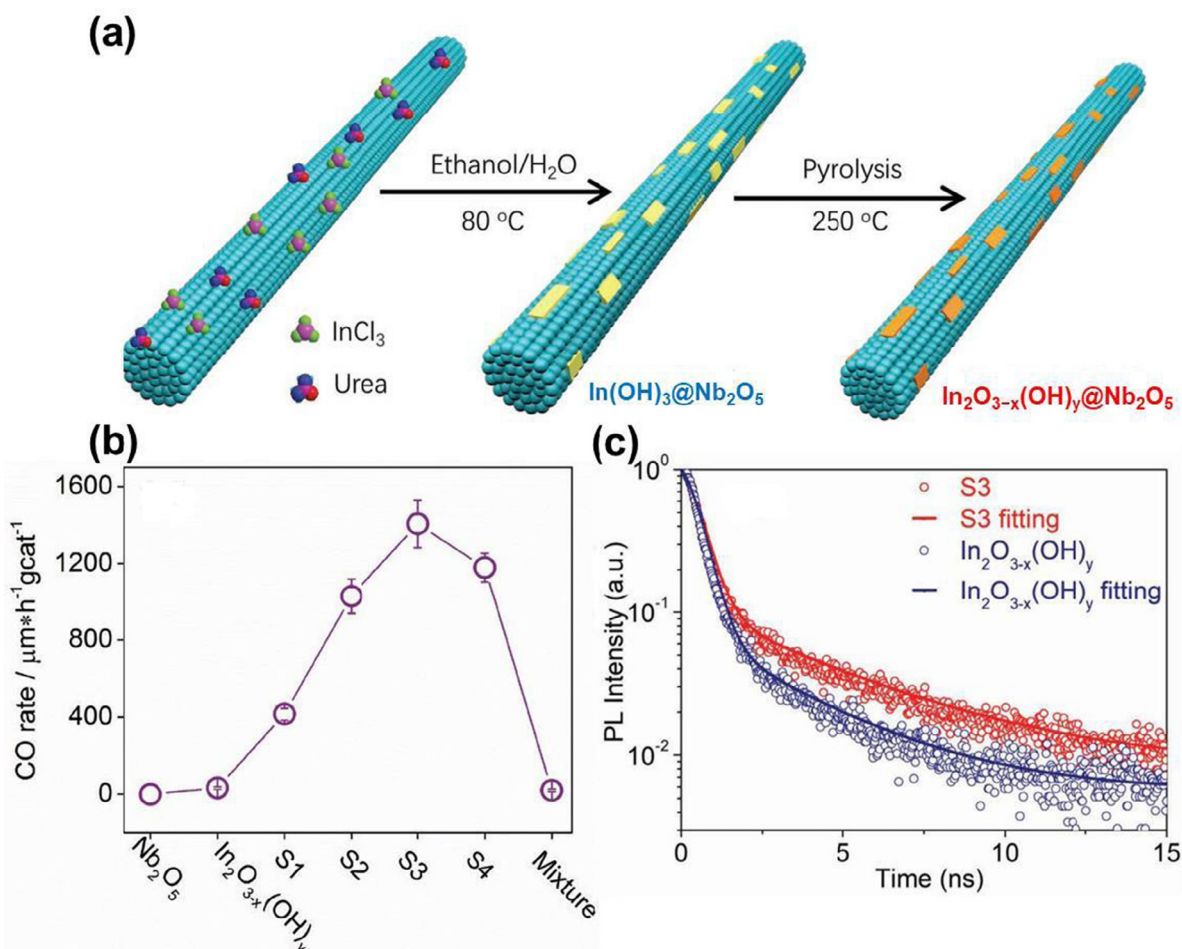


Fig. 5. (a) Schematic of the In<sub>2</sub>O<sub>3-x</sub>(OH)<sub>y</sub>@Nb<sub>2</sub>O<sub>5</sub> composite; (b) CO production rates for various samples; (c) fluorescence decay temporal profiles measured and fit for the optimized In<sub>2</sub>O<sub>3-x</sub>(OH)<sub>y</sub>@Nb<sub>2</sub>O<sub>5</sub> composite and pristine In<sub>2</sub>O<sub>3-x</sub>(OH). Reproduced with permission from Ref. [84].

last decade. To differentiate from these recent reviews, we focus on the utilization of different sustainable H<sub>2</sub> sources for the photoreduction of CO<sub>2</sub> to obtain value-added organic products. Various photocatalysts, photoreactor configurations, and reaction parameters for the photoreduction of CO<sub>2</sub> are discussed. For future research endeavors, a general approach for the photoreduction of CO<sub>2</sub> to mimic natural photosynthesis, in which the H<sub>2</sub> source is provided directly during the photocatalytic water splitting, is proposed and verified to successfully generate value-added organic products.

## 2. Photo-hydrogenation of CO<sub>2</sub> toward solar products

### 2.1. Understanding the roles and mechanism of H<sub>2</sub> sources

The mechanism of CO<sub>2</sub> photoreduction is complex. There has been intense debated regarding the roles of active H, including molecular H<sub>2</sub> and atomic H<sup>+</sup>, in the photoreduction of CO<sub>2</sub>. Instead of molecular H<sub>2</sub>, atomic H<sup>+</sup> has been proposed to photocatalyze CO<sub>2</sub> reduction via the proton-coupled multi-electron transfer processes, as follows [75]:



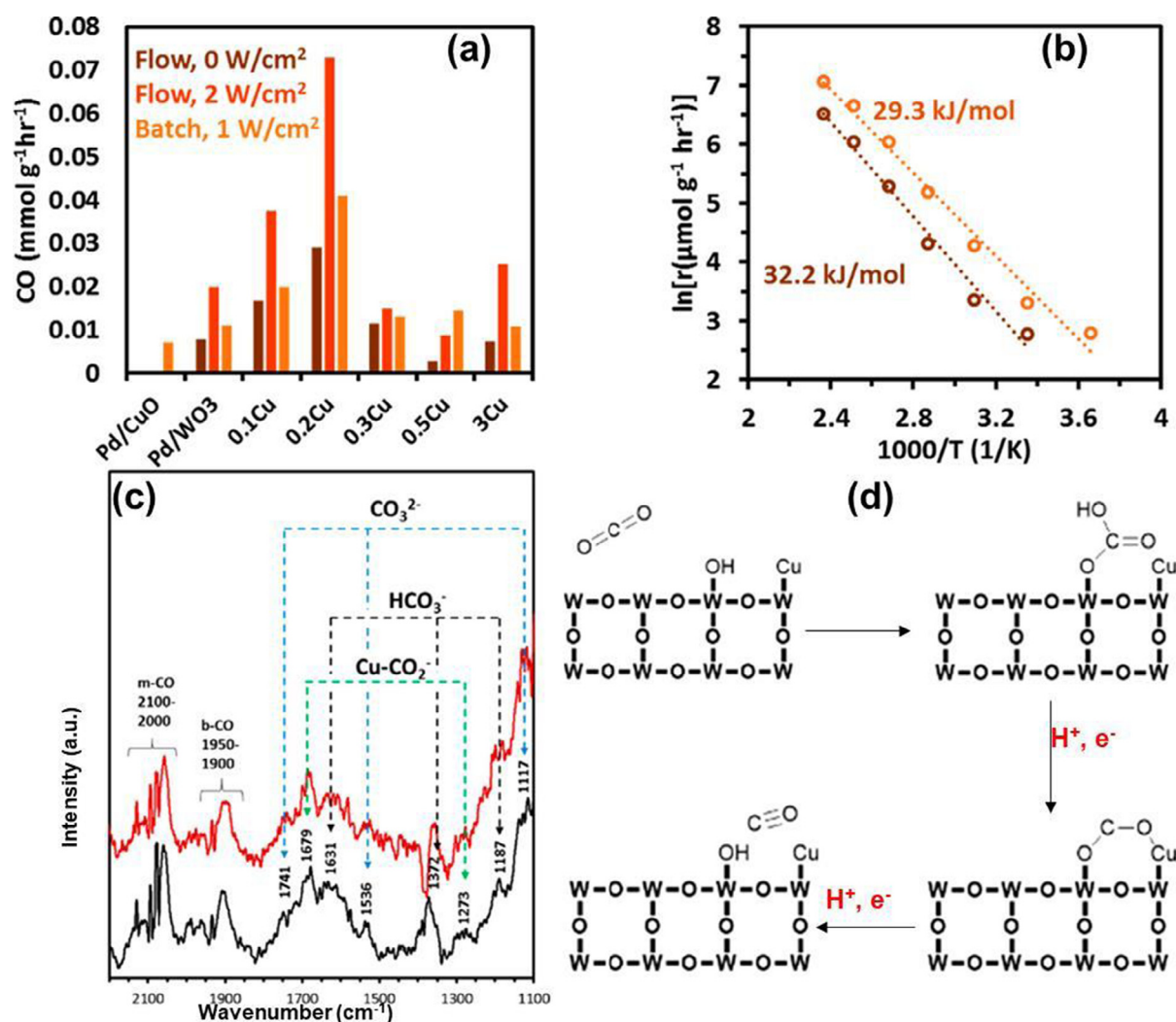
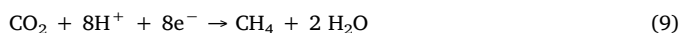
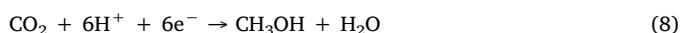
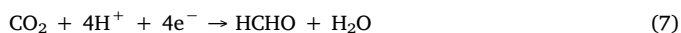
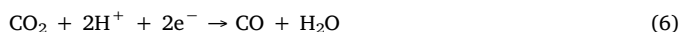


Fig. 6. (a) Light-assisted RWGS reaction for various samples; (b) Arrhenius plot for sample 0.2Cu in the dark (brown) and under illumination (orange); (c) DRIFTS of sample 0.2Cu in the dark (black) and under illumination (red); (d) proposed reaction pathway of CO formation over Cu-decorated Pd/WO<sub>3</sub>. Reproduced with permission from Ref. [93] (For interpretation of the references to colour in this figure legend, the reader is referred to the web version of this article.)



Li et al. performed an isotope experiment in a D<sub>2</sub>O, CO<sub>2</sub>, and H<sub>2</sub> atmosphere with Ru/NaTaO<sub>3</sub> for verifying whether the H<sub>2</sub> source was water (D<sub>2</sub>O) or H<sub>2</sub> in the products [49]. In the initial reaction, the H<sub>2</sub> in methane was mainly derived from water (D<sub>2</sub>O), with CD<sub>4</sub> as the primary product. Other products, including CD<sub>3</sub>H and CD<sub>2</sub>H<sub>2</sub>, were observed after several hours of the reaction. The results indicated that the active atomic H from the water source directly reduced CO<sub>2</sub> into solar products, while the molecular H<sub>2</sub> gas promoted the conversion of peroxide intermediates (O<sub>2</sub><sup>\*</sup>) into the water, as shown in Fig. 2.

According to the proton-coupled multi-electron transfer concept, Chen et al. successfully fused *Halobacterium* purple membrane-derived vesicles (PMVs) onto the surface of Pd-deposited porous hollow TiO<sub>2</sub> NPs (Pd-HTNPs), which were then employed for CO<sub>2</sub> photoreduction, as shown in Fig. 3a [75]. As expected, a well-defined core-shell structure was observed (Fig. 3b and 3c). As shown in Fig. 3d, CH<sub>4</sub> and CO were detected. For CH<sub>4</sub>, the production rate (56.4 μmol·g<sub>cat</sub><sup>-1</sup>·h<sup>-1</sup>) and selectivity (95.2%) were high. In blank tests in the absence of the

biohybrids (Pd-HTNPs@PMVs), light, or CO<sub>2</sub> (N<sub>2</sub> atmosphere), no catalytic performance was observed. The proton-coupled multi-electron transfer processes played an important role in the reduction of CO<sub>2</sub> into fuels and value-added chemicals, as shown in Fig. 3e.

As PtO<sub>x</sub> NPs have proven to be effective active sites for the direct splitting of water [76], PtO<sub>x</sub> NPs with a particle size of 2 nm were deposited on Bi<sub>2</sub>WO<sub>6</sub> nanosheets (Fig. 4b), which were then applied for the photoreduction of CO<sub>2</sub> into hydrocarbons [77]. As expected, the product yield initially increased with the PtO<sub>x</sub> loading; the optimal CH<sub>4</sub> production rate (108.8 ppm·g<sup>-1</sup>·h<sup>-1</sup>) was observed at 0.5%PtO<sub>x</sub> (Fig. 4a). Wang et al. confirmed the role of the proton-coupled multi-electron transfer processes in accelerating CO<sub>2</sub> photoreduction, as shown in Fig. 4c.

In addition to the H<sub>2</sub> source from water, molecular H<sub>2</sub>, or atomic H<sup>+</sup> intermediates [78], the idea to use H<sub>2</sub>-storage material to promote the photocatalytic reduction of CO<sub>2</sub> has received attention. Kang et al. reported that N<sub>2</sub>H<sub>4</sub>·H<sub>2</sub>O, which had a high content of H<sub>2</sub> (7.9%), effectively worked as the H<sub>2</sub> source and electron donor over Au<sub>3</sub>Cu@SrTiO<sub>3</sub>/TiO<sub>2</sub> nanotube arrays [64]. Based on this system, CH<sub>4</sub> was the primary product (an evolution rate of 421.2 μmol·g<sup>-1</sup>·h<sup>-1</sup>), which accounted 60% of the total hydrocarbon products. Interestingly, N<sub>2</sub>H<sub>4</sub>·H<sub>2</sub>O could generate a productive reductive atmosphere to protect and maintain the high stability of the Au<sub>3</sub>Cu@SrTiO<sub>3</sub>/TiO<sub>2</sub> nanotube

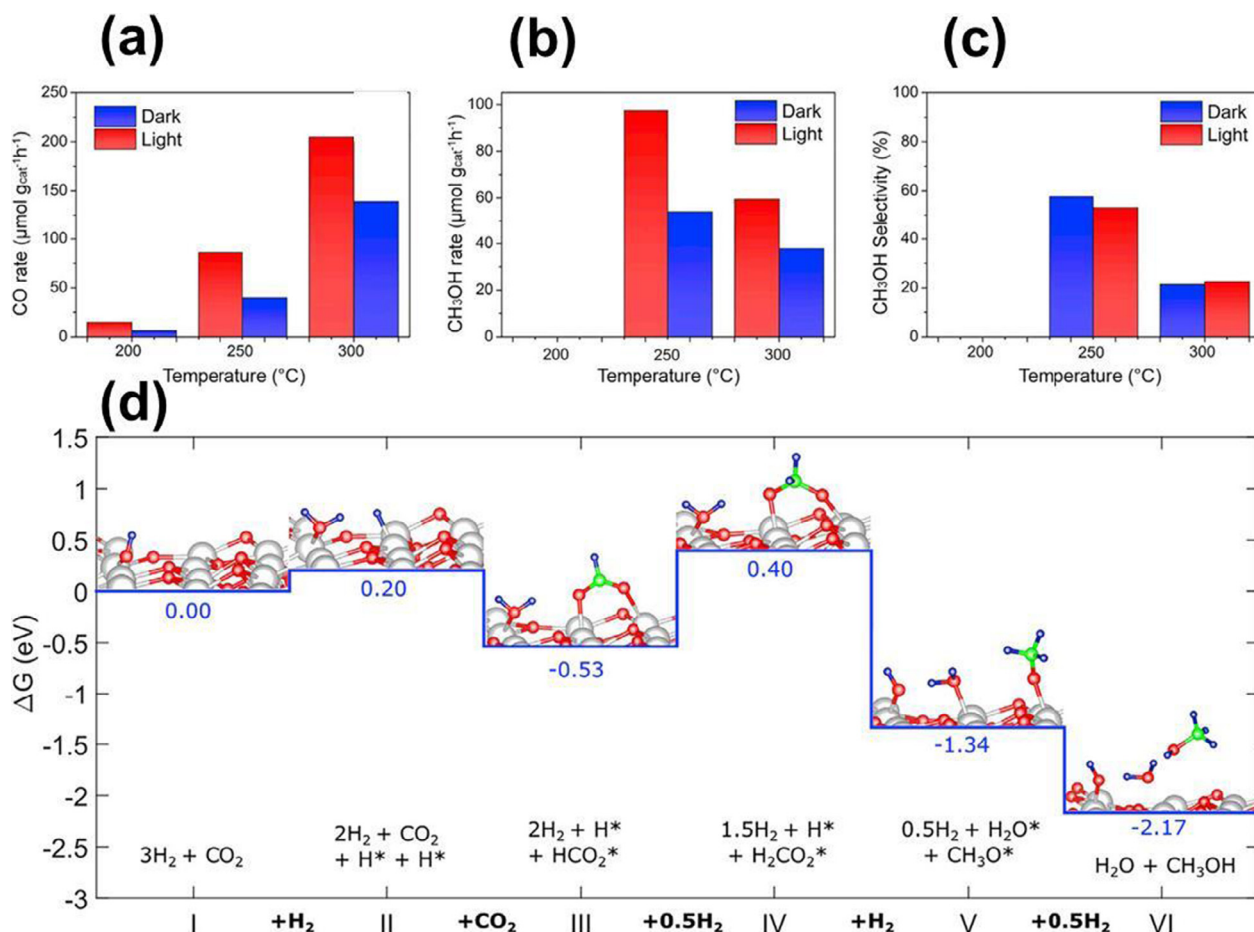


Fig. 7. Production of (a) CO and (b) CH<sub>3</sub>OH at three different temperatures; (c) CH<sub>3</sub>OH selectivity; (d) reaction pathway for CO<sub>2</sub>-to-CH<sub>3</sub>OH conversion. Reproduced with permission from Ref. [95].

arrays. As expected, the evolution rate of CH<sub>4</sub> still retained 87.6% of its original activity after five cycles of measurement during a 34 h test.

In summary, the concept of using H<sub>2</sub> source as reductants for CO<sub>2</sub> conversion might potentially impact solar fuel production. Many H<sub>2</sub> sources have been proposed, including water, molecular H<sub>2</sub>, H<sub>2</sub>-storage materials, or atomic H<sup>+</sup> intermediates, which could offer advantages of enhancing photocatalytic activity and prolonging their performances. It believes that these feasible routes would bring promising concepts on designing reaction conditions and developing photocatalysts to potentially promote the efficiency of photoreduction of CO<sub>2</sub>.

## 2.2. Photocatalysts

Photon-assisted CO<sub>2</sub> hydrogenation has attracted increasing attention in recent years. This method can efficiently convert CO<sub>2</sub> into high-value chemicals (e.g., CO, CH<sub>4</sub>, CH<sub>3</sub>OH, C<sub>2</sub>H<sub>4</sub>). It has considerable potential to address current CO<sub>2</sub> issues because the use of H<sub>2</sub> as the reductant significantly enhances the product yield [51,79]. In this section, the materials employed for four types of CO<sub>2</sub> conversion reactions—CO<sub>2</sub>-to-CO (reverse water-gas shift, RWGS), CO<sub>2</sub>-to-CH<sub>3</sub>OH, CO<sub>2</sub>-to-CH<sub>4</sub> (methanation reaction), and CO<sub>2</sub>-to-C<sub>2</sub>+ (hydrogenation reaction)—are discussed in detail.

### 2.2.1. Reverse water-gas shift

To date, many candidates have been highlighted as potential photocatalysts for photocatalytic hydrogenation of CO<sub>2</sub> [26]. Typically, In<sub>2</sub>O<sub>3</sub>-based catalysts are a promising candidate for the photocatalytic hydrogenation of CO<sub>2</sub>. Density functional theory (DFT) and time-dependent DFT calculations revealed that In<sub>2</sub>O<sub>3</sub> containing O vacancies is

favorable for the activation and hydrogenation of CO<sub>2</sub> [80,81]. Ghuman et al. reported that In<sub>2</sub>O<sub>3-x</sub>(OH)<sub>y</sub> consisting of surface hydroxide groups, and O vacancies facilitated photoinduced CO<sub>2</sub>-to-CO conversion. In<sub>2</sub>O<sub>3-x</sub>(OH)<sub>y</sub> catalysts promote the heterolytic dissociation of H<sub>2</sub>, which results in hydride- and proton-like H bonding to In atoms and the hydroxide group, respectively. Such as-formed species facilitate the interaction and electron transfer to the adsorbed CO<sub>2</sub> molecules [82]. In another study, He et al. prepared In<sub>2</sub>O<sub>3-x</sub>(OH)<sub>y</sub> nanorods to catalyze the solar-driven RWGS reaction (CO<sub>2</sub> + H<sub>2</sub> → CO + H<sub>2</sub>O) in a gas-phase medium. The In<sub>2</sub>O<sub>3-x</sub>(OH)<sub>y</sub> nanorod superstructure prepared via a two-step synthesis process prolonged the lifetime of photogenerated charge carriers owing to interparticle charge transfer. Owing to the unique properties of In<sub>2</sub>O<sub>3-x</sub>(OH)<sub>y</sub> and the nanorod superstructure comprising nanocrystals, the prepared In<sub>2</sub>O<sub>3-x</sub>(OH)<sub>y</sub> catalyst exhibited a significant enhancement in the light-assisted RWGS reaction [83]. Recently, Wang et al. constructed an In<sub>2</sub>O<sub>3-x</sub>(OH)<sub>y</sub>@Nb<sub>2</sub>O<sub>5</sub> heterostructure, which exhibited a superior improvement in the photoinduced RWGS reaction, as illustrated in Fig. 5. This nanocomposite was prepared via a simple two-step synthesis process involving the preparation of In(OH)<sub>3</sub>@Nb<sub>2</sub>O<sub>5</sub>, followed by calcination, to obtain an In<sub>2</sub>O<sub>3-x</sub>(OH)<sub>y</sub>@Nb<sub>2</sub>O<sub>5</sub> composite, as illustrated in Fig. 5a. The resulting heterostructure exhibited extraordinary performance in photocatalytic CO<sub>2</sub> reduction, as shown in Fig. 5b. The CO production rate was 44 times higher than that of pristine In<sub>2</sub>O<sub>3-x</sub>(OH)<sub>y</sub>. This improvement was due to the presence of O vacancies and hydroxides, as well as the heterostructure-induced prolonged charge-carrier lifetimes, as shown in Fig. 5c. The O vacancies and hydroxides functioned as reservoirs for photoexcited electrons and holes, respectively, whereas the heterostructure encouraged charge separation, stabilizing the excited states

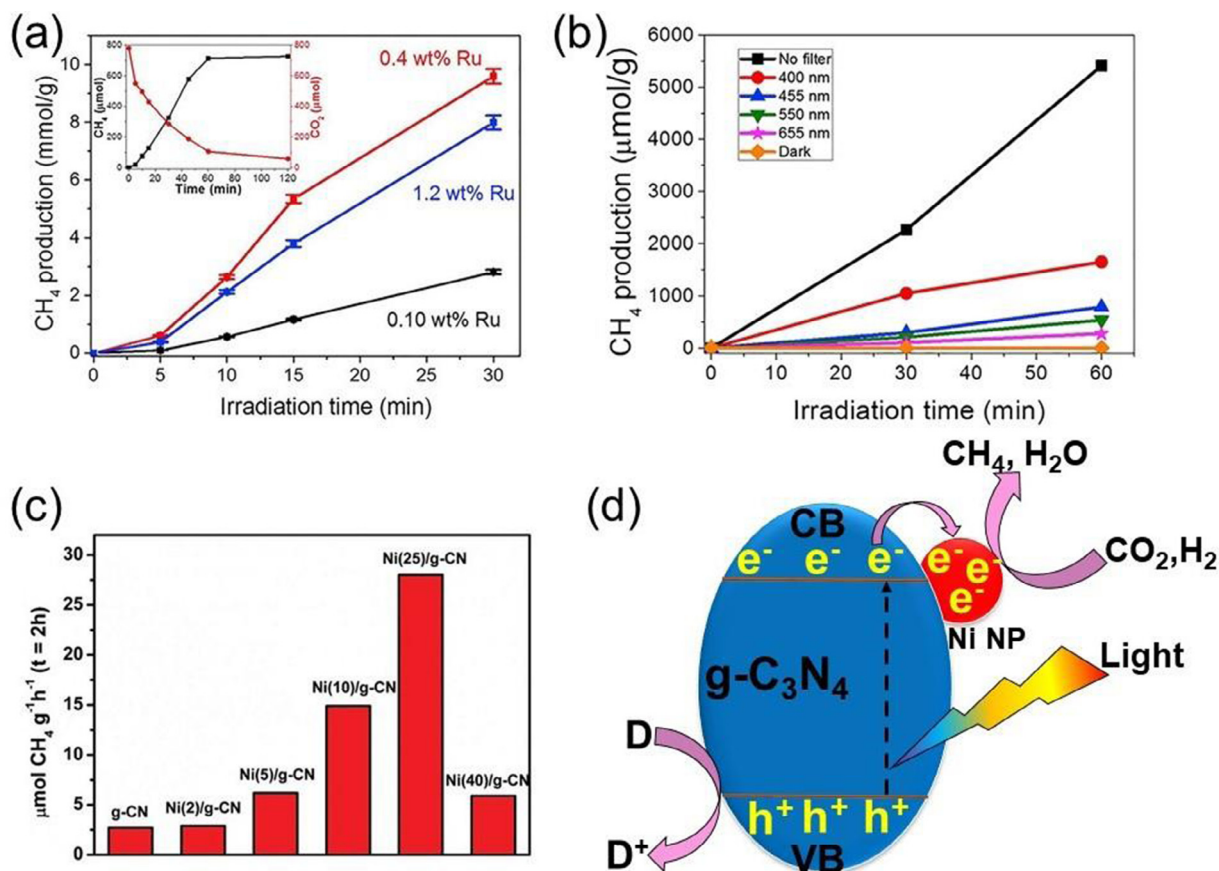


**Fig. 8.** Evolved  $\text{CH}_4$  over various  $\text{RuO}_2/\text{SrTiO}_3$  nanocomposites. (a) Different amounts of loaded Ru under the following conditions: a testing temperature of  $150\text{ }^\circ\text{C}$ ,  $1080\text{-W}\cdot\text{m}^{-2}$  illumination, and partial pressures of 1.05 and 0.25 bar for  $\text{H}_2$  and  $\text{CO}_2$ , respectively. The inset shows the  $\text{CO}_2$  and  $\text{CH}_4$  production (mmol) for the sample with 0.4 wt% Ru at  $150\text{ }^\circ\text{C}$ ;  $1000\text{-W}\cdot\text{m}^{-2}$  was applied using a 300-W Xe lamp. (b) Different illumination conditions. Reprinted with permission from Ref. [102]; Copyright 2019, Elsevier. (c) Photocatalytic  $\text{CH}_4$  formation of various Ni/g- $\text{C}_3\text{N}_4$  samples under the following conditions: a temperature of  $150\text{ }^\circ\text{C}$ ,  $1080\text{-W}\cdot\text{m}^{-2}$  illumination, and partial pressures of 1.05 and 0.25 bar for  $\text{H}_2$  and  $\text{CO}_2$ , respectively. Adapted with permission from Ref. [106]; Copyright 2019, Wiley. (d) Proposed formation of  $\text{CH}_4$  over Ni/g- $\text{C}_3\text{N}_4$  with the assistance of light and heat.

[84].

The use of metal nanoparticle (NP)/metal oxide catalysts arouses concern as the crucial approach in the RWGS reaction because metals induce the dissociation of  $\text{H}_2$ , whereas metal oxides offer a medium for  $\text{CO}_2$  adsorption and activation [85–87]. In this case, the irradiated light induces the generation of charge carriers, which can not only improve the dissociation of  $\text{H}_2$  but also reduce the activation barrier, enhancing the selectivity [86,88,89]. For example, Upadhye et al. investigated the activity of an Au/ $\text{TiO}_2$  nanocomposite for the RWGS reaction under visible light. The Au NP-incorporated  $\text{TiO}_2$  enhanced the  $\text{CO}_2$ -to- $\text{CO}$  performance owing to the decrease in the apparent activation energy from 47 to 35  $\text{kJ}\cdot\text{mol}^{-1}$  under irradiation. This improvement was explained by localized surface plasmon resonance-induced Au NPs, which enhanced the reaction kinetics [90]. Jia et al. reported that a Pd/ $\text{Ni}_2\text{O}_5$  nanocomposite was sufficient for the production of CO from  $\text{CO}_2$  and  $\text{H}_2$ . The enhanced activity originated from the photothermal effect of Pd “nanoheaters” generating heat. Moreover, numerous H atoms, which resulted from the dissociation of  $\text{H}_2$  on Pd nanocrystals and spillover to  $\text{Nb}_2\text{O}_5$  nanorods and were associated with the *in situ* formation of O vacancies and/or the reduced Nb oxidation state, significantly promoted the reaction between  $\text{CO}_2$  and  $\text{H}_2$  to produce CO [91]. In another study, the Pd/ $\text{H}_y\text{WO}_{3-x}$  heterostructure was demonstrated as an efficient catalyst for the light-assisted RWGS reaction. This enhancement was due to the coexistence of Brønsted acid hydroxyls OH, W(V) sites, and O vacancies ( $\text{V}_\text{O}$ ), which were achieved by a hydrogenation process. Notably, the Pd NPs decorated on  $\text{WO}_3$  significantly contributed to the formation of the defective structure of  $\text{WO}_3$  because they facilitated the

dissociation of  $\text{H}_2$  via spillover of H to the  $\text{WO}_3$  surface. Consequently, numerous modifications, such as Brønsted acid hydroxyls OH, W(V) sites, and O vacancies ( $\text{V}_\text{O}$ ), occurred. These outstanding properties reduced the apparent activation energy, along with the light irradiation. Therefore, a large amount CO could be produced over Pd/ $\text{H}_y\text{WO}_{3-x}$  [92]. In another study, by exploiting these features, Li et al. prepared a novel Cu-decorated nanowire Pd/ $\text{H}_y\text{WO}_{3-x}$  bronze heterostructure, representing a step toward improving the RWGS reaction. As shown in Fig. 6a, the presence of Cu on Pd/ $\text{WO}_3$  significantly increased the amount of CO produced in comparison with the sample prepared without Cu. Furthermore, the Cu-modified Pd/ $\text{WO}_3$  exhibited significantly lower activation energy for the production of CO (32.2  $\text{kJ}\cdot\text{mol}^{-1}$  in the dark and 29.3  $\text{kJ}\cdot\text{mol}^{-1}$  under illumination), suggesting efficient  $\text{CO}_2$ -to- $\text{CO}$  reduction over the Cu-modified Pd/ $\text{WO}_3$ , as shown in Fig. 6b. The Cu-modified Pd/ $\text{WO}_3$  promoted the reduction of  $\text{CO}_2$  via the formation of Cu-bound carboxylate intermediates, which was beneficial for the CO formation, as shown in Fig. 6c and 6d [93].

### 2.2.2. $\text{CO}_2$ -to- $\text{CH}_3\text{OH}$ conversion

The production of  $\text{CH}_3\text{OH}$  via  $\text{CO}_2$  hydrogenation ( $\text{CO}_2 + 3\text{H}_2 \rightarrow \text{CH}_3\text{OH} + \text{H}_2\text{O}$ ) is a critical obstacle because of (i) the competing RWGS reaction, (ii) the exothermic nature of the methanol formation reaction, and (iii) the high activation barrier [94]. Thus, the efficiency of the reaction is limited. Motivated by these challenges, in 2018, Wang et al. performed an extraordinary investigation into the  $\text{CO}_2$ -to- $\text{CH}_3\text{OH}$  conversion over  $\text{In}_2\text{O}_{3-x}(\text{OH})_y$  rod-like nanocrystals. The  $\text{CH}_3\text{OH}$  product

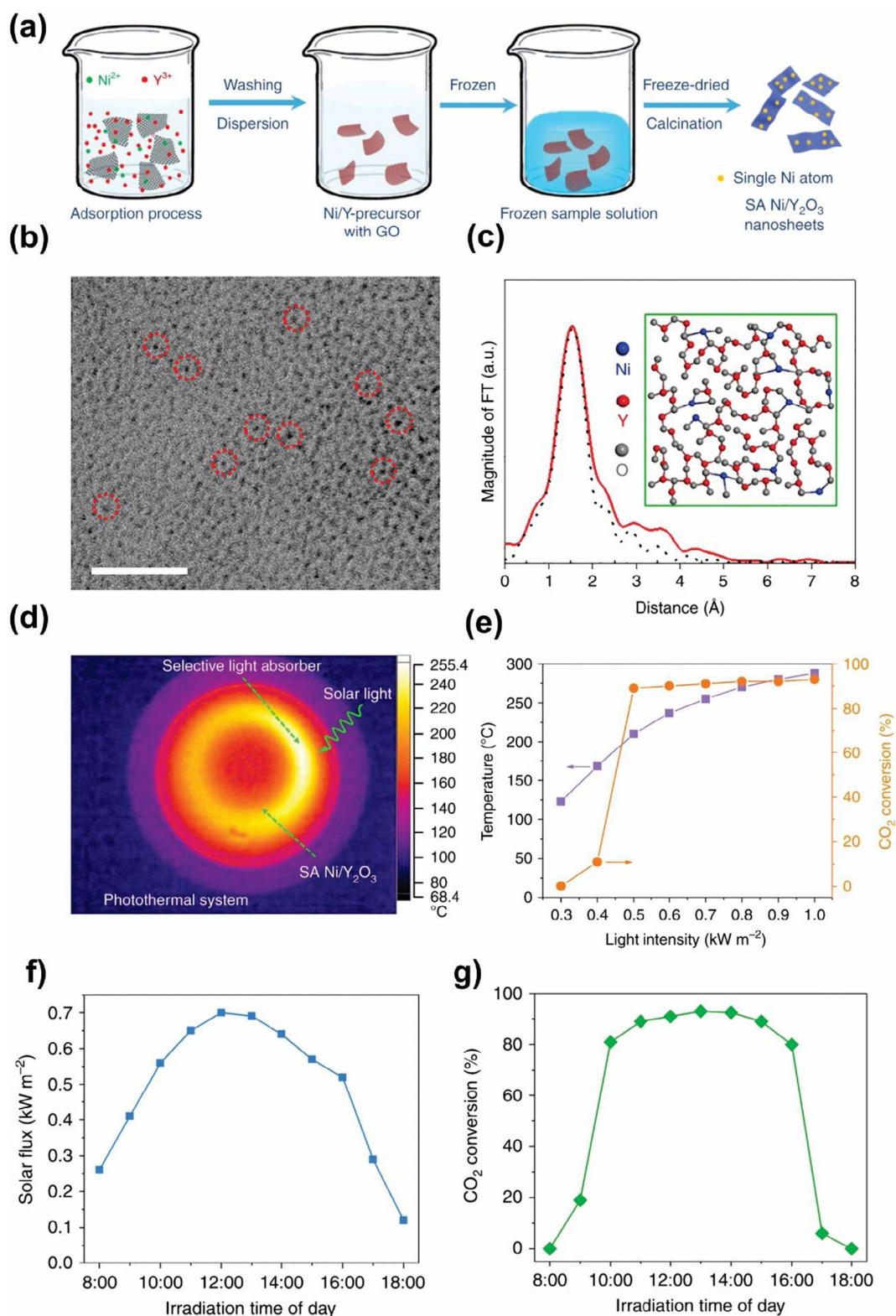


**Fig. 9.** (a) Schematic of the preparation of SA  $\text{Ni}/\text{Y}_2\text{O}_3$  nanosheets; (b) aberration-corrected TEM image of the SA  $\text{Ni}/\text{Y}_2\text{O}_3$  nanosheets; (c) schematic model of the SA  $\text{Ni}/\text{Y}_2\text{O}_3$  nanosheets and the corresponding FT-EXAFS fitting curves for the SA  $\text{Ni}/\text{Y}_2\text{O}_3$  nanosheets; (d) spatial temperature mapping obtained from the infrared camera under simulated solar light ( $1.0 \text{ kW m}^{-2}$ ), (e) temperature and  $\text{CO}_2$  conversion over the SA  $\text{Ni}/\text{Y}_2\text{O}_3$  nanosheets with respect to the light intensity; (f, g) solar flux and  $\text{CO}_2$  conversion at different times of the day. Reproduced with permission from Ref. [109].

was abundantly formed with the increasing hydrogenation temperature under light-assisted conditions. This was explained by the kinetic inhibition of the production of methanol at the low temperature and pressure, as shown in Fig. 7a-c. Notably, the amount of  $\text{CH}_3\text{OH}$

obtained via the hydrogenation approach was significantly higher than that for the best-known photocatalysts, indicating the potential of this method. Fig. 7d shows the reaction pathway for  $\text{CH}_3\text{OH}$  formation. Unique surface properties significantly impact the reaction pathway,

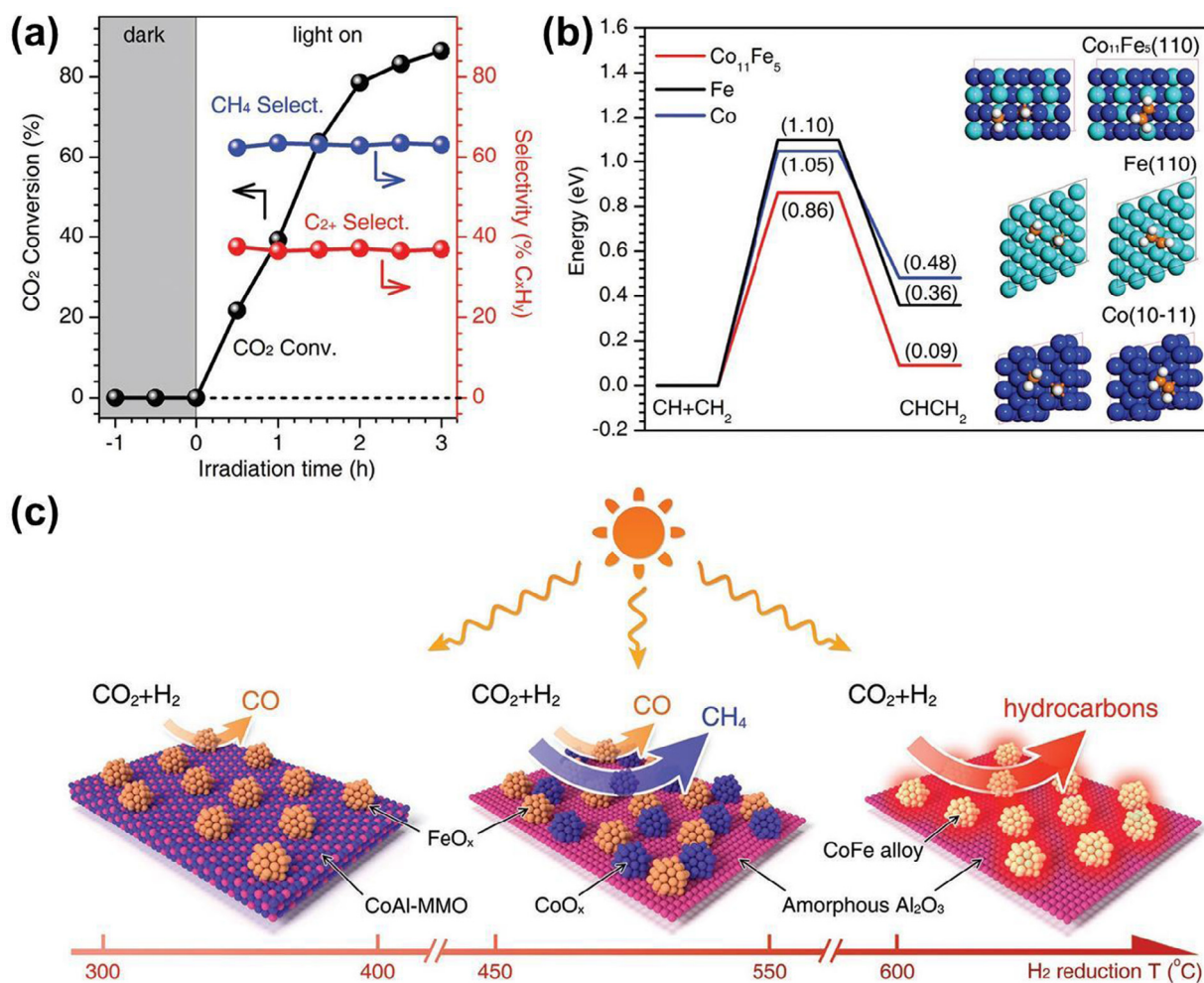


**Fig. 10.** (a) CO<sub>2</sub> conversion associated with the CH<sub>4</sub> and C<sub>2</sub>+ selectivity of the CoFe-650 sample under ultraviolet (UV)-visible irradiation; (b) DFT calculations for Co<sub>11</sub>Fe<sub>5</sub> (110), compared with Co (10-11), and Fe (110) configurations for the C-C coupling; (c) schematic of various samples treated at different H<sub>2</sub> reduction temperatures toward the selectivity of CO and hydrocarbons. Reproduced with permission from Ref. [121]

driving the formation of CH<sub>3</sub>OH. In this case, the irradiation strengthens the surface frustrated Lewis pairs, improving the reactivity for H<sub>2</sub> activation and reducing the activation barrier [95].

The hydrogenation of CO<sub>2</sub> to CH<sub>3</sub>OH is promising but rarely reported. Research in the field of catalysis is expended to grow significantly in the future, which can eventually lead to large-scale solar-driven CO<sub>2</sub>-to-fuel production.

### 2.2.3. CO<sub>2</sub>-to-methane (CH<sub>4</sub>) conversion

Considering the potential solar fuel of methane (CH<sub>4</sub>) and the environmental point of view of CO<sub>2</sub>, photo-hydrogenation of CO<sub>2</sub> to CH<sub>4</sub> has been proposed as a viable approach to producing high-value chemicals, which can be used for chemical storage [96]. Solar-driven production of CH<sub>4</sub> from CO<sub>2</sub> and H<sub>2</sub> is promising because it is eco-friendly and inexpensive [50,97,98]. However, the performance of the CO<sub>2</sub>-to-CH<sub>4</sub> reaction is limited, even though the reaction is thermodynamically favored (CO<sub>2</sub> + 4H<sub>2</sub> → CH<sub>4</sub> + 2H<sub>2</sub>O; ΔG<sub>298K</sub> = -130.8 kJ·mol<sup>-1</sup>). This reaction involves an eight-electron process, which is a significant kinetic restriction [99,100]. Therefore, the catalysts play an essential role in driving the reaction and increasing the amount of CH<sub>4</sub> produced. In the past decade, considerable effort has been directed toward the investigation of robust catalysts for solar-driven CO<sub>2</sub>-to-CH<sub>4</sub> hydrogenation [9,101-105]. The use of nanocomposites consisting of metal, metal oxide, and/or C-based materials is an attractive approach because the synergistic effects of the components significantly enhance the CO<sub>2</sub> adsorption, activation, and local

thermal effect, facilitating the CH<sub>4</sub> formation. For instance, Ren et al. used Ru-anchored ultrathin layered double hydroxides (LDHs) to promote photothermal CO<sub>2</sub> methanation. The Ru-LDHs composite was a very active catalyst for the formation of CH<sub>4</sub> from CO<sub>2</sub> under light irradiation, owing to the efficient CO<sub>2</sub> and H<sub>2</sub> activation [103]. Mateo et al. recently prepared a RuO<sub>2</sub>/SrTiO<sub>3</sub> heterostructure that significantly enhanced the generation of CH<sub>4</sub>. The RuO<sub>2</sub>-decorated SrTiO<sub>3</sub> exhibited high CH<sub>4</sub> production performance (up to 14.6 mmol·h<sup>-1</sup>·g<sup>-1</sup> in the optimized condition), as shown in Fig. 8a and 8b. This nanocomposite had a high CO<sub>2</sub> adsorption capacity because of the SrTiO<sub>3</sub>, and the local thermal effect at the Ru sites caused by charge separation and recombination was sufficient to drive the methanation reaction on the Ru NPs [102].

Recently, there are some candidates have been proposed for selective photoreduction of CO<sub>2</sub>, which offer various advantages, including low-cost materials, high chemical/thermal stability. In typical, Barrio et al. recently reported the methanation of CO<sub>2</sub> using a Ni/g-C<sub>3</sub>N<sub>4</sub> nanocomposite synthesized from supramolecular, followed by Ni<sup>2+</sup> impregnation and H<sub>2</sub> treatment. Fig. 8c shows the evolved CH<sub>4</sub> from various g-C<sub>3</sub>N<sub>4</sub> and Ni/g-C<sub>3</sub>N<sub>4</sub> samples, indicating the superior CH<sub>4</sub> formation over the Ni/g-C<sub>3</sub>N<sub>4</sub> composite compared with the pristine g-C<sub>3</sub>N<sub>4</sub>. The optimized sample—Ni(25)/g-CN—produced CH<sub>4</sub> with a rate of 28 μmol·g<sup>-1</sup>·h<sup>-1</sup>, which was approximate ~ 10.3 times higher than that of the g-CN sample [106]. This outstanding activity originated from the efficient charge-carrier separation and transportation from g-C<sub>3</sub>N<sub>4</sub> to Ni NPs. The generated electrons easily migrated from g-CN to

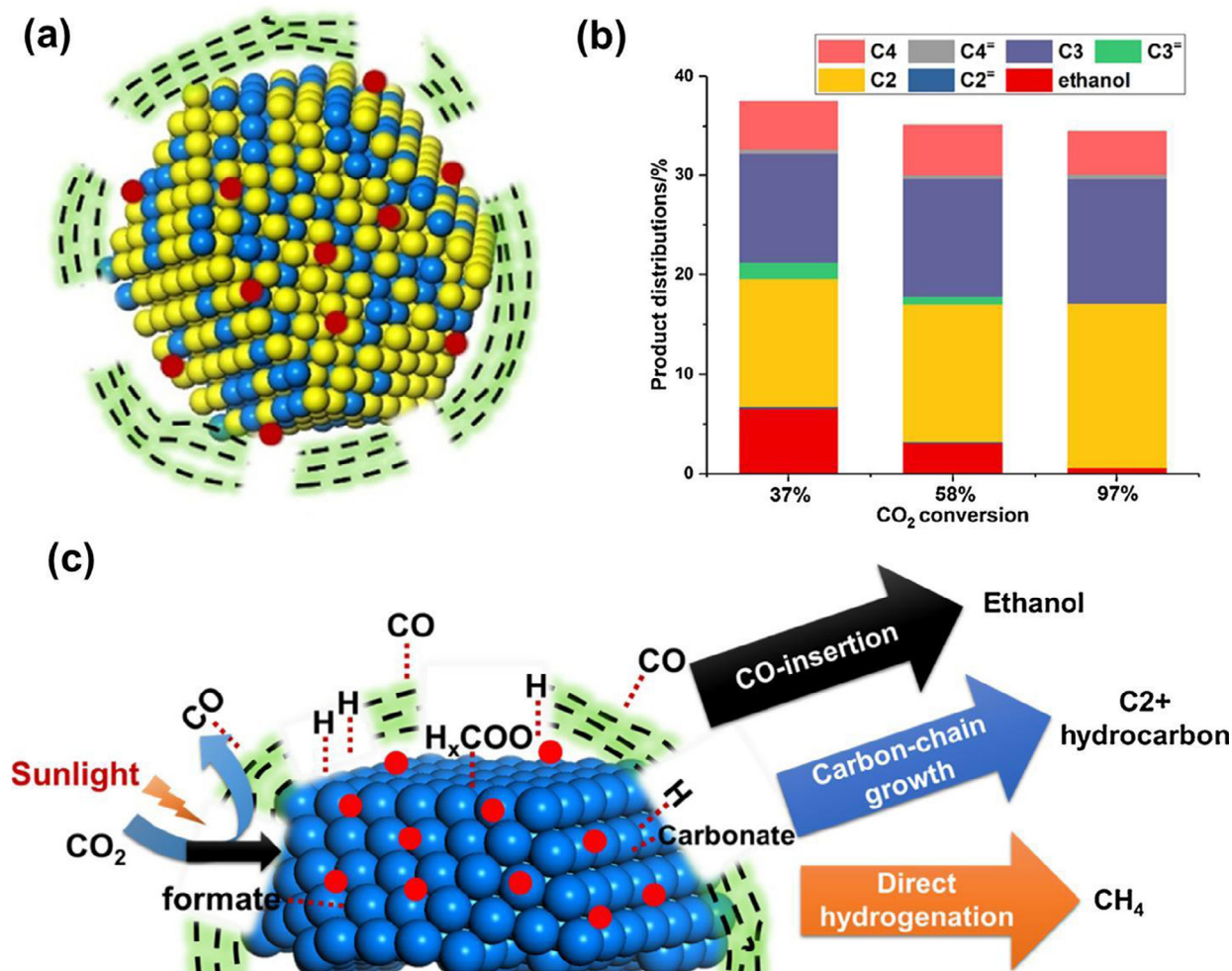


**Fig. 11.** (a) Schematic of the Na-Co@C structure; (b) selectivity of C<sub>2+</sub> products under the photothermal condition over Na-Co@C at different CO<sub>2</sub> conversion rates; (c) schematic of the formation of CH<sub>4</sub> and C<sub>2+</sub>. Reproduced with permission from Ref. [122].

Ni species, resulting in electron-rich reactive sites with an improved affinity for CO<sub>2</sub> and H<sub>2</sub>. These advantages associated with the high reaction temperature improved the reactivity and methane formation, as shown in Fig. 8d [106]. In another study, Tahir et al. successfully designed montmorillonite (Mt) coupled with modified g-C<sub>3</sub>N<sub>4</sub> (m-CN) 2D/2D hybrid composite [107], oxygen-defective OV-Ti<sub>3</sub>AlC<sub>2</sub> with proton-rich functionalized carbon nitride (f-C<sub>3</sub>N<sub>4</sub>) [108], for CO<sub>2</sub> reduction to fuels. They found that the CO and CH<sub>4</sub> yield rate could reach to 253 and 165 μmol·g<sup>-1</sup>·h<sup>-1</sup>, respectively, over Mt/g-C<sub>3</sub>N<sub>4</sub> photocatalyst. Photocatalytic conversion CO<sub>2</sub>-to-CH<sub>4</sub> is a promising valuable source of renewable energy. Recently, the findings of metals free graphitic carbon nitride (g-C<sub>3</sub>N<sub>4</sub>), metal carbides compounds (MAX) materials, has opened a very bright future to develop non-noble metal catalysts for the light-driven methanation of CO<sub>2</sub>.

Reducing the size of Ni species to a Ni cluster or a single atom (SA) is expected to result in extraordinary performance for CH<sub>4</sub> generation. In this aspect, the efficiency of Ni can be improved while reducing the amount of loaded Ni species. Li et al. recently prepared single Ni atom catalyst-anchored ultrathin amorphous Y<sub>2</sub>O<sub>3</sub> nanosheets exhibiting a superior CO<sub>2</sub>-to-CH<sub>4</sub> conversion ability. The preparation of the SA Ni/Y<sub>2</sub>O<sub>3</sub> nanosheet composites involved three steps, as shown in Fig. 9a. Graphene oxide (GO) was utilized as a support for the Ni<sup>2+</sup> and Y<sup>2+</sup> ion adsorption caused by the interaction between metal ions and GO prior to the freeze-drying and calcination. The Ni SAs were uniformly decorated on the Y<sub>2</sub>O<sub>3</sub> nanosheets, as shown in Fig. 9b. In the SA Ni-Y<sub>2</sub>O<sub>3</sub> nanosheets (Fig. 9c), the Ni SAs formed Ni-O bonds with neighboring O

atoms of Y<sub>2</sub>O<sub>3</sub>. These bonds stabilized the Ni SAs, restricting their aggregation into Ni NPs during the calcination step. The temperature under simulated solar light (1.0 kW·m<sup>-2</sup>) was as high as ~ 255 °C (Fig. 9d). Furthermore, the temperature of the SA Ni/Y<sub>2</sub>O<sub>3</sub> nanosheets under the assistance of a selective light absorber (AlN<sub>x</sub>/Al foil) reached 285 °C under 1.0 kW·m<sup>-2</sup> when the gas inlet and outlet were encapsulated by thermal insulating covers, as shown in Fig. 9e. In this condition, the CO<sub>2</sub> conversion rate approached 90%, with very high CH<sub>4</sub> selectivity. These results indicate the extraordinary catalytic CO<sub>2</sub> methanation of the SA Ni-Y<sub>2</sub>O<sub>3</sub> nanosheets. Fig. 9f and 9 g show the solar flux and the CO<sub>2</sub> reduction performance concerning the irradiation time (time of day). The Ni/Y<sub>2</sub>O<sub>3</sub> nanosheets exhibited superior CO<sub>2</sub> conversion under natural sunlight, suggesting that this composite is promising for solar-driven CO<sub>2</sub> methanation [109]. These results indicate the outstanding properties of materials containing SA catalysts. The preparation of single metal atom-supported metal oxides will be a popular research topic in the coming years. Various candidates for metal SA catalysts and numerous supports can be selected to promote CO<sub>2</sub> adsorption, activation, and reduction and enhance the product selectivity. Therefore, plenty of room will be waiting for the exploration of superior catalysts in this research field in the coming years.

Graphene-based catalysts have been sufficient for the preparation of highly active materials for the light-driven production of CH<sub>4</sub> from CO<sub>2</sub> and H<sub>2</sub>. This is due to the unique properties of graphene, e.g., the extended π orbital, high thermal and electrical conductivities, and large specific surface area, which are beneficial for CO<sub>2</sub> adsorption and

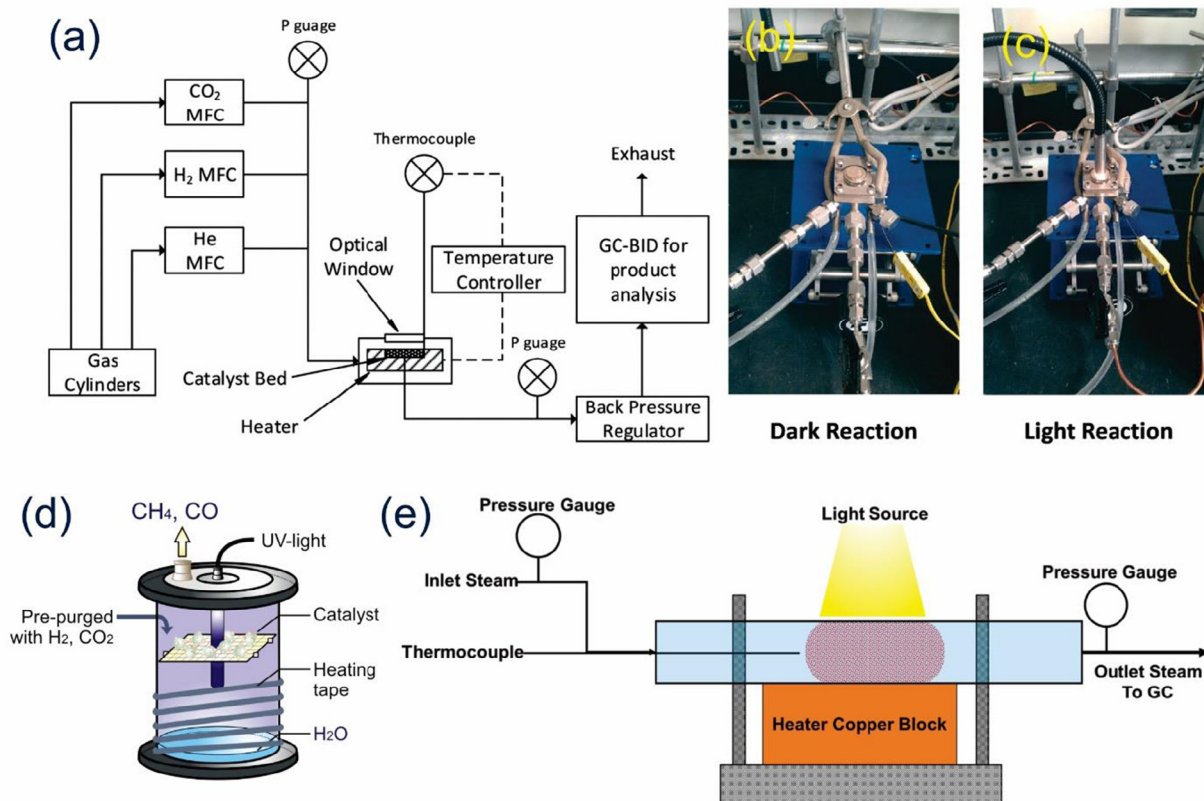


Fig. 12. (a) Schematic of a typical batch-type reactor; (b, c) corresponding photographs captured under dark and light conditions. Reproduced with permission from Ref. [90]. (d) Fixed-bed photoreactor Reproduced with permission from Ref. [9]. (e) Illustration of a flow reactor. Reproduced with permission from Ref. [82].

reduction [101,110–112]. Therefore, the preparation of graphene-based composites has attracted research attention [113–115]. For instance, NiO/Ni NP-supported graphene exhibited a significant improvement in the CO<sub>2</sub> methanation performance compared with Ni NPs supported on large-surface area silica-alumina. Graphene facilitated the charge transfer from NiO/Ni to graphene sheets, while the high reaction temperature reduced the adsorption of H<sub>2</sub>O molecules, which negatively affected the catalytic performance [104].

#### 2.2.4. Hydrogenation of CO<sub>2</sub> into C<sub>2+</sub> products

The conversion of CO<sub>2</sub> into ethanol and C<sub>2+</sub> hydrocarbons is an attractive topic because of the higher value and energy density of C<sub>2+</sub> products compared with C<sub>1</sub> products [116–118]. However, the generation of C<sub>2+</sub> products is challenging, owing to the C–C coupling reaction. The intermediates should have the appropriate binding energy for binding to the catalyst surface to promote the C–C coupling reaction [117,119–121]. Therefore, the photocatalyst surface plays a crucial role in driving the reaction, leading to the formation of C<sub>2+</sub> with high selectivity. In 2018, Chen et al. reported the hydrogenation of CO<sub>2</sub> into high-value products via an alumina-supported CoFe alloy catalyst, which was fabricated via the hydrogenation of CoFeAl LDH nanosheets [121]. The optimum catalyst treated at 650 °C (denoted as CoFe-650) exhibited an evolved C<sub>2+</sub> product with high selectivity, along with a methane product, as shown in Fig. 10a. In this case, the formation of the CoFe alloy was considered as the primary factor driving the CO<sub>2</sub> hydrogenation that formed C<sub>2+</sub> hydrocarbons. DFT calculations (Fig. 10b) revealed that the CoFe surface provided a lower barrier to adsorbed CH–CH<sub>2</sub> than the Co and Fe surfaces, indicating that the CoFe alloy promoted the C–C coupling reaction. This approach provides a novel pathway for the rational design of the hydrogenation of CO<sub>2</sub> into high-value chemical products, as shown in Fig. 10c [121].

In another study, Liu et al. found that a Na-Co@C nanocomposite had a robust capability for the photocatalytic production of C<sub>2+</sub> hydrocarbons and ethanol (Fig. 11a). In this case, UV light played an essential role in the generation of electrons, which were accumulated in C species. The electron-rich C species activated CO<sub>2</sub> into CO<sub>2</sub><sup>δ-</sup>, and CO<sub>2</sub> was dissociated into CO, driving the formation of ethanol. Importantly, the as-generated CO was stabilized by the C layer on the catalyst surface, while the Na affected the intermediate species, promoting the C–C formation. Such surface features are imperative for the formation of C<sub>2+</sub> products, as shown in Fig. 11a–c [122].

In the other approach, the use of Co-based catalysts appears to provide a pathway to obtain C<sub>2+</sub> products in light-assisted CO<sub>2</sub> hydrogenation. It is crucial to stabilize the CO intermediate on the catalyst surface to promote the C–C coupling reaction. Furthermore, the catalyst surface with a moderate amount of C<sub>2+</sub> products is beneficial for desorption, which can enhance the selectivity. In this context, Cu-based materials are potential candidates, as they have proven to be useful for hydrogenation and electrocatalytic CO<sub>2</sub> reduction [123–128].

Research on the production of C<sub>2+</sub> chemicals will become increasingly popular in the coming years. To date, various candidates, including CoFe-based catalysts, Na-Co@C nanocomposite, Co-based catalysts, Cu-based catalysts, have been successfully prepared and demonstrated as a novel photocatalytic material platform to produce valuable chemicals and fuels from CO<sub>2</sub>. From the present data, how to accumulate the charge carriers effectively and protons play a vital role to favor the formation of C<sub>2+</sub> products. These investigations are expected to unveil the nature of photocatalysts and provide extraordinary materials for enhancing C<sub>2+</sub> production via photocatalytic hydrogenation of CO<sub>2</sub>.

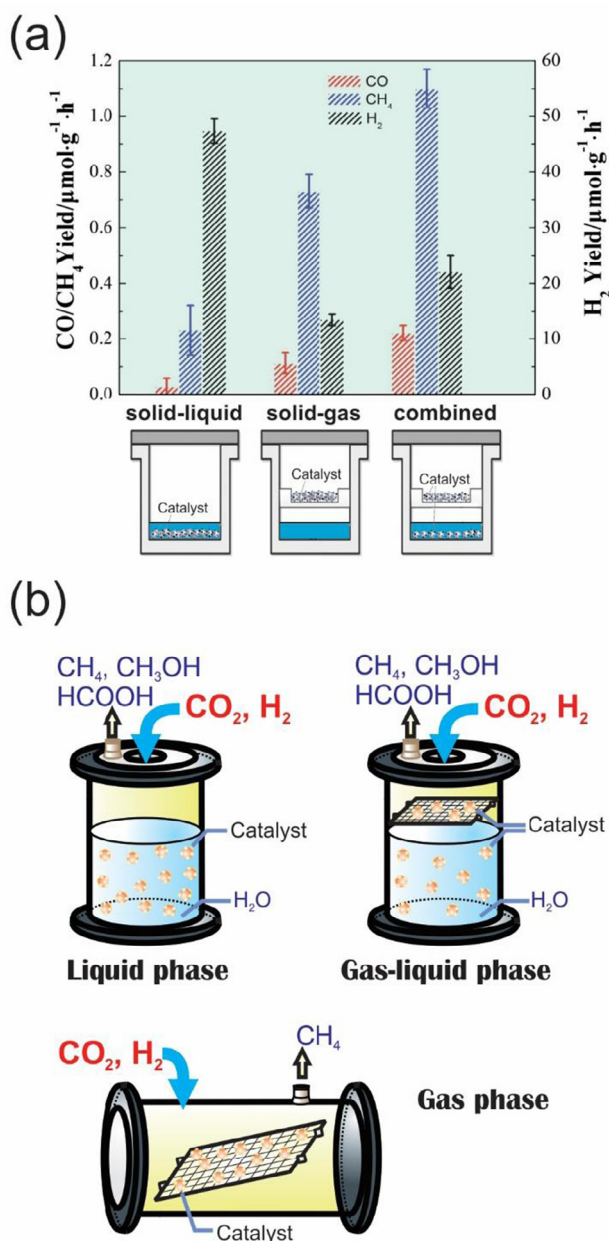


Fig. 13. (a) Photocatalytic hydrogenation/reduction of CO<sub>2</sub> over the Pt/TiO<sub>2</sub> photocatalyst with different reaction modes. Reproduced with permission from Ref. [130]. Three reaction modes were conducted for CO<sub>2</sub> photo-hydrogenation. Reproduced with permission from Ref. [11].

### 2.3. Photoreactor design

It notes that the efficiency of photohydrogenation of CO<sub>2</sub> is still relatively low. Hence, several factors, such as light distribution, reaction mode, product separation, and geometries of the reactor, have gained considerable attention. These factors lead to further design and develop novel photoreactors to enhance the photocatalytic hydrogenation of CO<sub>2</sub> performances [8,11].

Two general types of reactors—batch- and flow-type—have been developed to perform the CO<sub>2</sub> photohydrogenation reaction. Fig. 12a–c describes a typical batch-type reactor system for photocatalytic CO<sub>2</sub> hydrogenation. This system consists of gas suppliers, reactors, and analyzer sections. It allows *in situ* product analysis, and the temperature can be controlled. Therefore, both thermal- and light-assisted hydrogenation of CO<sub>2</sub> can be performed in this system [90,129]. Another

fixed-bed photoreactor (385 mL in volume) is designed by Chen et al., which is applied for the photohydrogenation of CO<sub>2</sub> in the presence of both H<sub>2</sub>O (liquid phase) and H<sub>2</sub> (gas phase), as displayed in Fig. 12d [9]. Herein, the photocatalyst powder is evenly placed on a flat Teflon surface, which is fixed in the middle of the photoreactor. The advantages of bath-type photoreactor are simple construction and operation, low-cost for a large-scale photoreactor. However, it frequently causes undesired second reactions or decompositions. To minimize this drawback, flow reactors have been employed in various solar-driven CO<sub>2</sub> hydrogenation studies and have achieved promising results. Fig. 12e shows a typical design of a capillary flow-type reactor. This configuration prolongs the reactant–catalytic surface interaction time, as the gas reactants travel through the capillary reactor [82]. Another advantage of the continuous flow-type could offer accurate control of the irradiation time, light irradiation via the flow rate.

In summary, several types of photoreactor have been proposed for photohydrogenation of CO<sub>2</sub> to produce solar fuels. It is noting that some of the parameters and operating conditions, such as temperature, light distribution, reaction mode, and product separation, offer critical roles in promoting yield and selectivity to products. Although many efforts have been devoted to designing photoreactors, low surface-to-volume ratios, and inefficient light distribution are still the primary concerns. Therefore, further researches require special attention to upgrade the geometrical design of the radiation source to reaction space and improve the ratio of illuminated-light surface area to volume of photoreactor.

### 2.4. Influence of reaction mode on photocatalytic activity

Xiong et al. reported that the reaction mode (solid–liquid, solid–gas, and combined solid–liquid–gas, as shown in Fig. 13a) can influence the photocatalytic activity of Pt/TiO<sub>2</sub>. For example, the solid–liquid mode enhances the formation of H<sub>2</sub> (H<sub>2</sub>: 47.3  $\mu\text{mol}\cdot\text{g}_{\text{cat}}^{-1}\cdot\text{h}^{-1}$ ; CO: 0.03  $\mu\text{mol}\cdot\text{g}_{\text{cat}}^{-1}\cdot\text{h}^{-1}$ ; CH<sub>4</sub>: 0.23  $\mu\text{mol}\cdot\text{g}_{\text{cat}}^{-1}\cdot\text{h}^{-1}$ ), while the solid–gas mode promotes the reduction of CO<sub>2</sub> (H<sub>2</sub>: 13.4  $\mu\text{mol}\cdot\text{g}_{\text{cat}}^{-1}\cdot\text{h}^{-1}$ ; CO: 0.11  $\mu\text{mol}\cdot\text{g}_{\text{cat}}^{-1}\cdot\text{h}^{-1}$ ; CH<sub>4</sub>: 0.73  $\mu\text{mol}\cdot\text{g}_{\text{cat}}^{-1}\cdot\text{h}^{-1}$ ) [130]. As expected, combining the solid–liquid and solid–gas modes can significantly promote the photo-hydrogenation of CO<sub>2</sub>, yielding the highest CO and CH<sub>4</sub> production rates (H<sub>2</sub>: 22.1  $\mu\text{mol}\cdot\text{g}_{\text{cat}}^{-1}\cdot\text{h}^{-1}$ ; CO: 0.22  $\mu\text{mol}\cdot\text{g}_{\text{cat}}^{-1}\cdot\text{h}^{-1}$ ; CH<sub>4</sub>: 1.1  $\mu\text{mol}\cdot\text{g}_{\text{cat}}^{-1}\cdot\text{h}^{-1}$ ). In this mode, the H<sub>2</sub> generated by the solid–liquid interface reaction promotes the photoreduction of CO<sub>2</sub> through the solid–gas reaction. In another study, Chen et al. did a study on three types of reaction mode, including a gas-phase, a liquid-phase, and a gas–liquid-phases, correspondingly (as shown in Fig. 13b) [11]. They found that the combined gas–liquid phases showed a remarkable result ( $1.1 \times 10^{-3}\%$  in quantum efficiency), whereas the efficiency levels of the gas- and liquid-phase systems were only  $0.1 \times 10^{-3}\%$  and  $0.5 \times 10^{-3}\%$ , respectively. The observation of efficiency enhancement might be contributed by the effective utilization of both H<sub>2</sub> in the gas phase and the atomic H<sup>+</sup> in the liquid phase. Although the experiments were carried out in different reaction modes (such as gas, liquid, gas–liquid phases), their photocatalytic mechanisms would not be changed [11]. However, the presence of photocatalysts in different reaction modes might boost reactions toward different reaction pathways.

## 3. Photoreduction of CO<sub>2</sub> for mimicking natural photosynthesis

Since the early pioneering work of Inoue et al. [44], the photo-hydrogenation of CO<sub>2</sub> has received significant attention. However, in these studies, an electron donor (H<sub>2</sub> gas) had to be continuously introduced to the reaction system. To mimic the natural photosynthesis in green plants, artificial photosynthesis using molecular H<sub>2</sub> or atomic H<sup>+</sup>, which is directly produced by photocatalytic water splitting, for the photoreduction of CO<sub>2</sub> has recently attracted increasing attention. Various promising photocatalytic semiconductor materials and

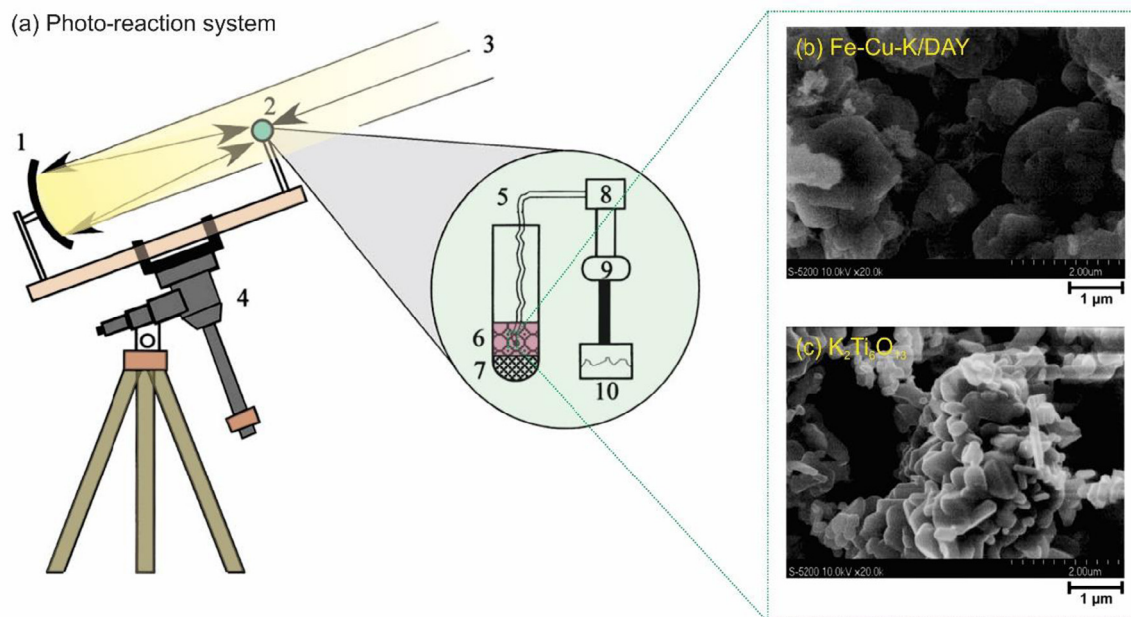


**Fig. 14.** (a) Experimental setup for the photo-hydrogenation of  $\text{CO}_2$  using a concentrated sunlight system: (1) concave mirror; (2) reaction cell; (3) sunlight; (4) GPD-type equatorial mount; (5) thermocouple; (6) photocatalysts; (7) quartz wool; (8) temperature compensator; (9) NR-1000 data-acquisition system; (10) laptop computer. Scanning electron microscopy images of the (b) Fe-Cu-K/DAY photocatalyst and (c)  $\text{K}_2\text{Ti}_6\text{O}_{13}$  photocatalyst. Reproduced with permission from Ref. [66].

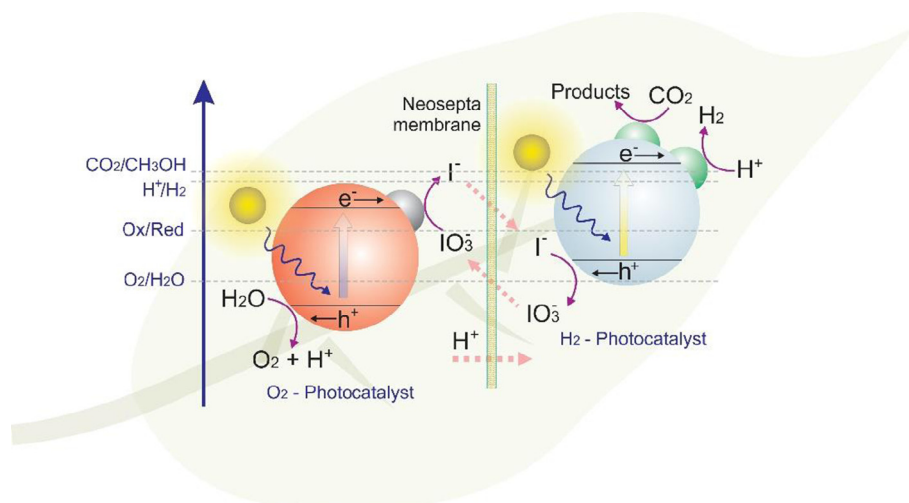


**Fig. 15.** Combination of  $\text{H}_2\text{O}$  water splitting and  $\text{CO}_2$  photo-hydrogenation in a Z-scheme system to mimic the natural photosynthesis process in green plants. (For interpretation of the references to colour in this figure legend, the reader is referred to the web version of this article.)

concepts to facilitate the production of solar fuels have been investigated.

In 2003, Guan et al. proposed the use of  $\text{H}_2$  from water splitting for the photo-hydrogenation of  $\text{CO}_2$  with hybrid photocatalysts under concentrated sunlight, as shown in Fig. 14a [66]. The photoreaction was conducted between 9:30 AM to 03:30 PM on sunny days (Oct. to Dec. 2001), which concentrated solar irradiation, providing effective photons and high thermal energy (average reaction temperature: 534–590 K; solar insolation:  $3.73\text{--}6.06 \text{ kWh}\cdot\text{m}^{-2}$ ). In this system, the  $\text{Pt}/\text{K}_2\text{Ti}_6\text{O}_{13}$  and Fe-Cu-K/DAY (Fe-Cu-K/dealuminized Y-type zeolite) photocatalysts were cubic particles (approximately  $0.5\text{--}2.0 \mu\text{m}$ , Fig. 14b) and rod-like crystallites (Fig. 14c), respectively. The role of the  $\text{Pt}/\text{K}_2\text{Ti}_6\text{O}_{13}$  photocatalyst was to split water into  $\text{H}_2$ , and that of the Fe-Cu-K/DAY photocatalyst was to hydrogenate  $\text{CO}_2$  into organic compounds, including methane ( $\text{CH}_4$ ,  $0.037\text{--}0.047 \mu\text{mol}\cdot\text{g}_{\text{cat}}^{-1}\cdot\text{h}^{-1}$ ), formic acid ( $\text{HCOOH}$ ,  $0\text{--}12.93 \mu\text{mol}\cdot\text{g}_{\text{cat}}^{-1}\cdot\text{h}^{-1}$ ), formaldehyde ( $\text{HCHO}$ ,

$0\text{--}3.43 \mu\text{mol}\cdot\text{g}_{\text{cat}}^{-1}\cdot\text{h}^{-1}$ ), methanol ( $\text{CH}_3\text{OH}$ ,  $0\text{--}4.83 \mu\text{mol}\cdot\text{g}_{\text{cat}}^{-1}\cdot\text{h}^{-1}$ ), and ethanol ( $\text{C}_2\text{H}_5\text{OH}$ ,  $0\text{--}1.17 \mu\text{mol}\cdot\text{g}_{\text{cat}}^{-1}\cdot\text{h}^{-1}$ ). However, the yield of these products was not attractive and required further improvement.

Recently, a novel twin photoreactor, which was designed according to the Z-scheme concept, was proposed to mimic the natural photosynthesis process in green plants, as shown in Fig. 15 [131]. This photocatalytic reactor system is separated by a circular membrane that consists of two different photocatalytic materials—e.g.,  $\text{Pt}/\text{SrTiO}_3\text{:Rh}$  combined with  $\text{Pt}/\text{CuAlGaO}_4$ , and  $\text{WO}_3$  [132], dual-function  $\text{GaN}:\text{ZnO}/\text{Ni}/\text{NiO}$  and  $\text{Pt}/\text{WO}_3$  [12],  $\text{Pt}/\text{TiO}_2$  and  $\text{Cu}/\text{TiO}_2$  [133], or  $\text{Pt}/\text{CuAlGaO}_4$  combined with  $\text{Pt}/\text{SrTiO}_3\text{:Rh}$  and  $\text{WO}_3$  [10,134]—for  $\text{CO}_2$ -hydrogenation/ $\text{H}_2$ -generation and  $\text{O}_2$ -generation, respectively, and integrates with different reversible shuttle redox mediators, e.g.,  $\text{IO}_3^-/\text{I}^-$  [12] or  $\text{Fe}^{2+}/\text{Fe}^{3+}$  [10,132]. This concept has many advantages. First, the  $\text{O}_2$  and  $\text{H}_2$ /solar products generated separately in the twin photoreactor via water splitting effectively hinder the backward reaction and

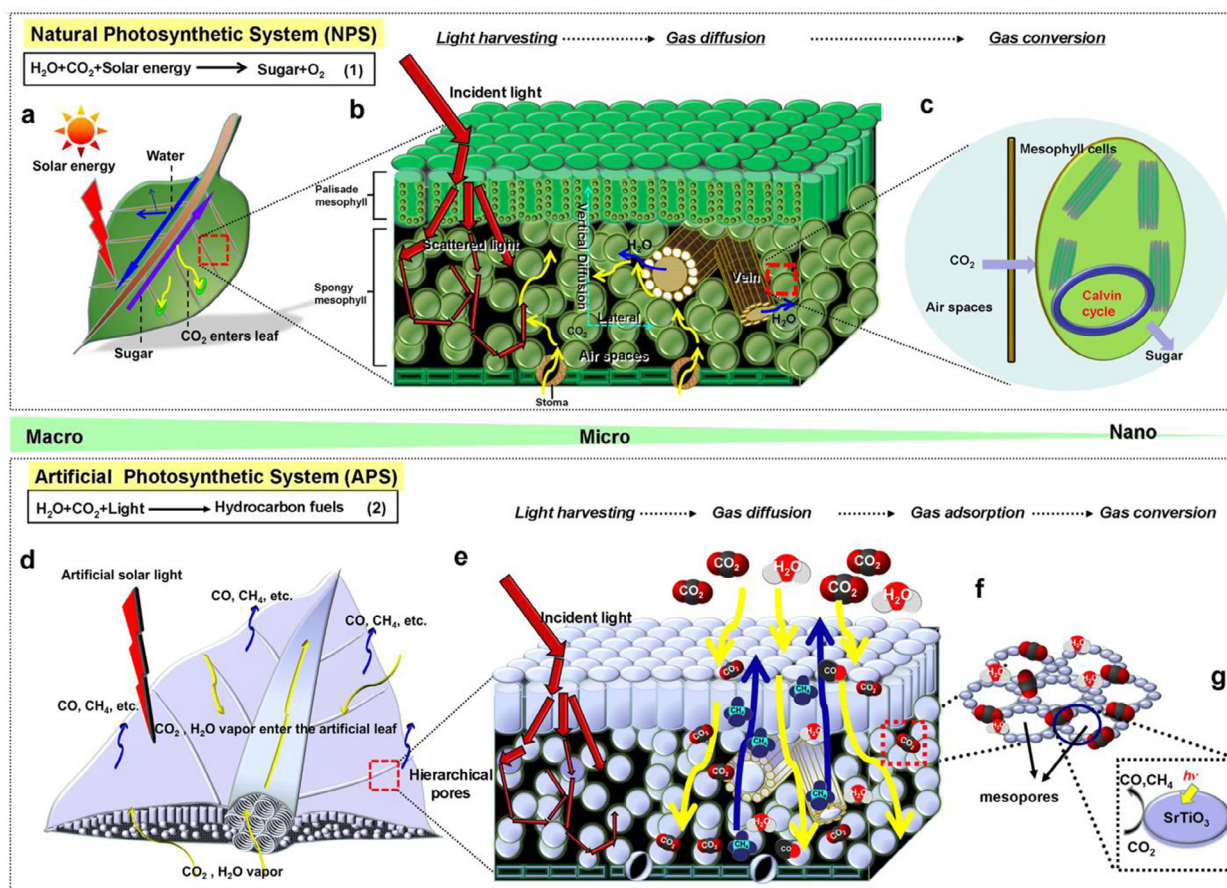


**Fig. 16.** Schematics of the NPS and APS: (a) Green leaf at the macroscale. (b) Light harvesting and gas diffusion in the NPS at the microscale. (c) Gas conversion at the nanoscale. (d) Artificial leaf at the macroscale. (e) Light harvesting and gas diffusion in the APS at the microscale. (f) Gas adsorption in the APS at the nanoscale. (g) Gas conversion in the APS at the nanoscale. Reproduced with permission from Ref. [136]. (For interpretation of the references to colour in this figure legend, the reader is referred to the web version of this article.)

oxidation of hydrocarbon products. Second, molecular H<sub>2</sub> and atomic H<sup>+</sup>, which are directly produced by the photocatalytic water splitting, are straightforwardly used for effective CO<sub>2</sub> hydrogenation.

Various experimental and theoretical studies on twin photoreactors for CO<sub>2</sub> have been conducted. Lee et al. reported that the performance of a dual-photocatalyst system in which Pt/SrTiO<sub>3</sub>-Rh and Pt/CuAlGaO<sub>4</sub> were used as H<sub>2</sub>-generation and CO<sub>2</sub>-reduction photocatalysts, respectively, was more than twice that of a single-photocatalyst system [132]. Recently, Yu et al. proposed a dual-function GaN:ZnO-Ni/NiO photocatalyst with both CO<sub>2</sub>-reduction and H<sub>2</sub>-production capabilities [12]. Interestingly, the photoreduction quantum efficiency of the twin photoreactor was more than four times higher than that of a single photoreactor (an increase from 0.015% to 0.070%). In another approach, Chu et al. proposed a novel bubbling twin photoreactor on the basis of theoretical calculations [135]. The results indicated that the diffusion and mass transfer between the gas and liquid phases were significantly improved, resulting in a higher conversion efficiency compared to the traditional twin photoreactor.

To summarize, a combination of H<sub>2</sub>O water splitting and CO<sub>2</sub> photohydrogenation in a Z-scheme system is successfully explored and adopted by using the novel twin photoreactor system to mimic the natural photosynthesis process in green plants. To date, various photocatalytic materials, which are integrated with different reversible shuttle redox mediators, perform significantly photoreduction quantum efficiency, selectivity for CO<sub>2</sub> reduction, diffusion, and mass transfer between the gas and liquid phases via twin photoreactor, in compared with single photoreactor. Currently, the bottleneck of this system is limited by the H<sub>2</sub>-generating efficiency, leading to develop the novel

H<sub>2</sub>-photocatalysts further.

#### 4. The prototype of an artificial leaf to mimic the unique structure of a leaf

The design of an artificial leaf that mimics the unique structure of a leaf has significant potential for the reduction of CO<sub>2</sub> emissions and the development of renewable fuels. Zhou et al. proposed a prototype artificial leaf for the photoreduction of CO<sub>2</sub> into hydrocarbon fuels, as shown in Fig. 16 [136]. The typical natural photosynthetic system (NPS) at multiple scales is depicted in Fig. 16a–c. At the macroscale, green leaves produce O<sub>2</sub>, carbohydrates, and other C-rich products by splitting H<sub>2</sub>O and reducing CO<sub>2</sub> in the presence of solar energy (Fig. 16a). At the microscale, the structures of the leaves function effectively to exchange gas, transport H<sub>2</sub>O, and harvest solar light (Fig. 16b). At the nanoscale, CO<sub>2</sub> can efficiently diffuse throughout the mesophyll cells, where it may dissociate into carbohydrates and other C-rich products (Fig. 16c). By developing a special design for artificial leaves, which include perovskite titanates (ATiO<sub>3</sub>, A = Sr, Ca, and Pb), an artificial photosynthetic system (APS) that mimics real leaves and employs only renewable resources, such as solar light and water, for photoreduction of CO<sub>2</sub> into hydrocarbon fuels, was proposed, as shown in Fig. 16d–g [136,137].

However, the efficiency of the APS is relatively low, and further research is required. The overall design of artificial leaves should comprehensively consider the geometries of leaf for optimizing solar light harvesting, exchanging gas, transporting H<sub>2</sub>O, photocatalytic materials (type, morphology, composition, and support). Meanwhile,

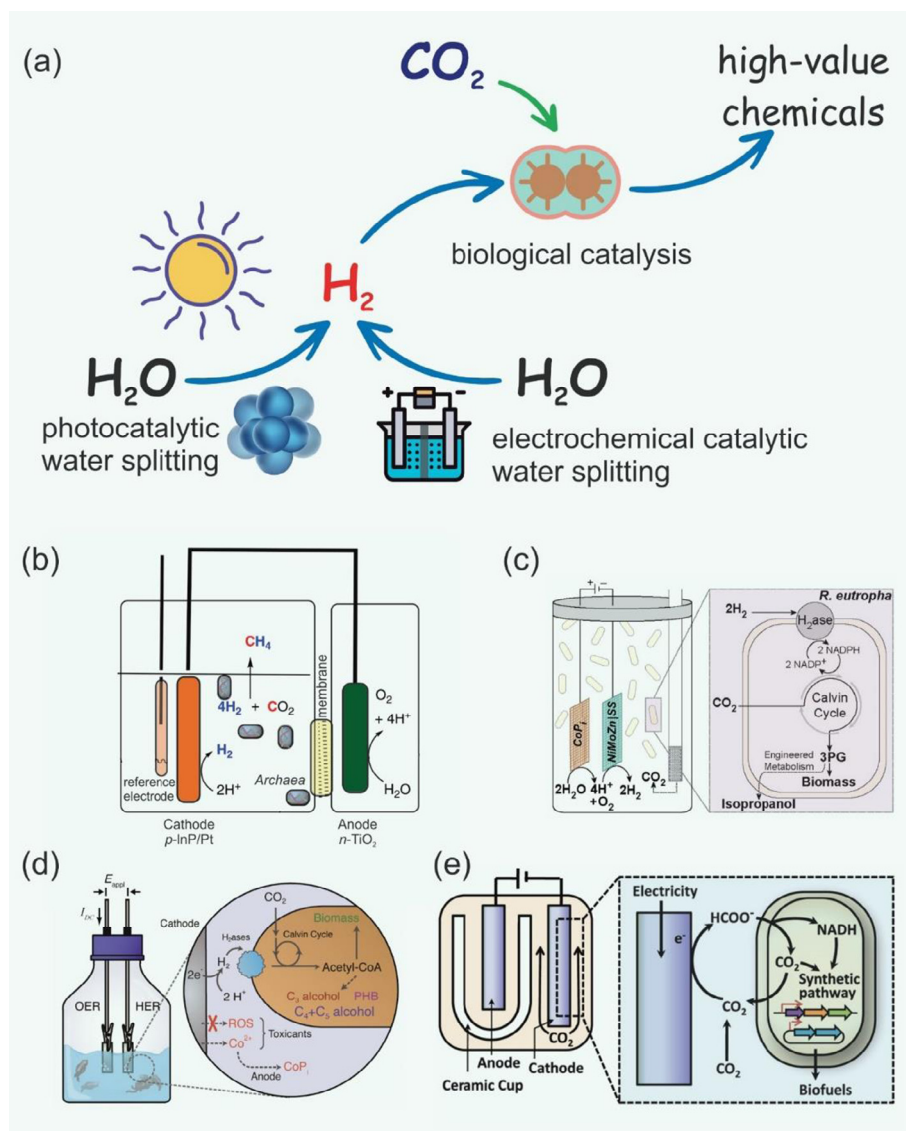


**Fig. 17.** (a) Hybrid photoelectrochemical biological approach for solar-to-chemical conversion. (b) Schematic of the generalized electrolytic setup, showing the *in situ* generation of  $H_2$  at the cathode followed by  $H_2$ -driven reduction of carbon dioxide to methane by the *M. barkeri* biocatalyst. (c) Bioelectrochemical cell for  $CO_2$  fixation. Reproduced with permission from Ref. [140]. (d) Hybrid bioelectrochemical system to convert  $CO_2$  into higher alcohols. Reproduced with permission from Ref. [141]. (e) Integrated electromicrobial process for  $CO_2$  fixation. Reproduced with permission from Ref. [142].

special attention should also focus on enhancing durability and extend the lifetime of modularized artificial leaf units for the potential industrialization.

### 5. Hybrid photoelectrochemical biological approach for solar-to-chemical conversion

One promising approach that was recently proposed is the development of a hybrid photoelectrochemical biological system in which photocatalytic materials are combined to drive water splitting and microbial fixation of  $CO_2$  into biomass and liquid fuels, as shown in Fig. 17a [138]. This sustainable concept uses only sustainable electrical and/or solar inputs to sustainably generate  $H_2$  from water, and then, the  $H_2$  is used with microorganisms to transform  $CO_2$  into high-value chemicals.

In typical, Nichols et al. reported an electrochemical cell that contains two chambers: cathodic and anodic chambers (Fig. 17b) [139]. In the cathodic chamber, the *p*-InP cathode electrochemically generated  $H_2$ , which was subsequently used *in situ* by *Methanosarcina barkeri* to reduce  $CO_2$  to  $CH_4$ . In the anodic chamber,  $O_2$  was produced separately

to prevent harmful potential by reactive O species. The conversion rate (*in situ* generations of  $H_2$  at the cathode) reached 86%, followed by an  $H_2$ -driven reduction of carbon dioxide to methane by the *Methanosarcina barkeri* biocatalyst. As shown in Fig. 17c, Torella et al. designed a bioelectrochemical cell [140] containing a cobalt phosphate (CoPi) anode and a nickel molybdenum zinc (NiMoZn) cathode to generate  $O_2$  and  $H_2$  via water splitting.  $H_2$  was used to efficiently convert  $CO_2$  via the Calvin cycle into biomass in wild-type *Ralstonia eutropha* H16 and to isopropanol in an engineered strain of *Ralstonia eutropha*, Re2133-PEG12. The solar-to-biomass yields and the isopropanol reached 3.2% and 216  $mg \cdot L^{-1}$ , respectively. However, this approach is a temporary solution owing to its limitations, including the low solubility, low mass transfer rate, and safety issues of the generated  $H_2$  in the microbial cultures. For reducing the toxicity to the bacterium, Liu et al. proposed a hybrid bioelectrochemical system for  $CO_2$  fixation (as shown Fig. 17d) [141], which could effectively minimize the generation of toxically reactive O species. The *R. eutropha* hybrid system achieved  $\eta_{SCE}$  values of 9.7%, 7.6%, and 7.1% for biomass, bioplastic, and liquid fuels (C3, C4, and C5 alcohols), respectively. Another approach is to electrochemically produce formate, instead of  $H_2$  and then convert it into

biofuels (isobutanol, 3-methyl-1-butanol, etc.) via a biological pathway (Fig. 17e) [142].

A concept of a hybrid photoelectrochemical biological system, which uses electrical and/or solar inputs to sustainably generate H<sub>2</sub> from water, and then, the H<sub>2</sub> is used with microorganisms to transform CO<sub>2</sub> into high-value chemicals, represents a significant breakthrough. However, this approach still requires further studies to enhance the efficiency of achieving sustainable solar-to-chemical energy conversion.

## 6. Conclusions and future perspectives

In conclusion, the conversion of CO<sub>2</sub> into valuable chemicals and renewable fuels associated with H<sub>2</sub> utilization has emerged as a mainstream approach to address the overwhelming CO<sub>2</sub> pollution. This research field can grow significantly in the future. In this review, four promising approaches for light-driven CO<sub>2</sub> reduction were identified: (i) the development of robust catalysts for light-assisted CO<sub>2</sub> hydrogenation, (ii) the mimicking of natural photosynthesis, (iii) the preparation of an artificial leaf, and (iv) the use of hybrid bioinorganic systems.

The hydrogenation of CO<sub>2</sub> has proven to be an efficient method of reducing CO<sub>2</sub>. The selection of materials significantly affects the outcomes. This review identified the following critical reactions: RWGS, CO<sub>2</sub>-to-CH<sub>3</sub>OH, methanation (CO<sub>2</sub>-to-CH<sub>4</sub>), and CO<sub>2</sub>-to-C<sub>2+</sub> conversion. The preparation of novel and inexpensive materials to increase the efficiency of each type of reaction is imperative. Research on the generation of C<sub>2+</sub> products, which are very high-value chemicals, is still in an early stage. The synthesis of extraordinary catalysts that reduce the working temperature and enhance the selectivity will facilitate the practical reduction of CO<sub>2</sub>.

Mimicking natural photosynthesis is another outstanding route for converting CO<sub>2</sub> into high-value chemicals. In this method, a photocatalytic system is employed, and the reaction medium (e.g., solid-liquid, solid-gas, combined systems) and material designs significantly affect the conversion efficiencies. It is expected that innovative reactor designs and extraordinary materials will lead to enhancements in the CO<sub>2</sub> conversion performance with regard to conversion and selectivity. A reactor design that has outstanding properties and overcomes the limitations of current designs is highly needed. Additionally, the development of active and durable photocatalysts with a strong reduction capability will help to fill the current large gap in CO<sub>2</sub> conversion and inspire research on high-performance and low-cost materials for solar-driven CO<sub>2</sub> reduction.

The preparation of an artificial leaf is also an intensive approach to convert CO<sub>2</sub> owing to the unique structure of the leaf, which can promote light-harvesting, mass transfer, and gas diffusion. Notably, the integrated technique plays a crucial role in the preparation of an efficient leaf, and the use of efficient catalysts promotes the reduction reaction. It is believed that new techniques, e.g., three-dimensional printing, will lead to the development of leaves with unique structures for CO<sub>2</sub> conversion.

Hybrid photoelectrochemical biological systems have considerable potential for efficient solar-driven CO<sub>2</sub>-to-fuel conversion. The critical issues regarding the solubility, mass transfer, and safety can be considered as the primary obstacles to be addressed. Solving these problems will present an excellent opportunity for the large-scale production of renewable solar fuels from CO<sub>2</sub>. We believe that our review provides a roadmap for the future solar-driven CO<sub>2</sub> reduction into high-value chemicals.

## Declaration of Competing Interest

The authors declare that they have no known competing financial interests or personal relationships that could have appeared to influence the work reported in this paper.

## Acknowledgements

This work is funded by the Creative Materials Discovery Program through the National Research Foundation of Korea (NRF) funded by the Ministry of Science and ICT [grant number 2017M3D1A1039379], the Basic Research Laboratory of the NRF funded by the Korean government [grant number 2018R1A4A1022647] and the Korea Research Fellowship Program through the NRF funded by the Ministry of Science and ICT [grant number 2020H1D3A1A04081409].

## Appendix A. Supplementary data

Supplementary data to this article can be found online at <https://doi.org/10.1016/j.cej.2020.126184>.

## References

- [1] S.C. Roy, O.K. Varghese, M. Paulose, C.A. Grimes, Toward Solar Fuels: Photocatalytic Conversion of Carbon Dioxide to Hydrocarbons, *ACS Nano* 4 (2010) 1259–1278.
- [2] M.R. Hoffmann, J.A. Moss, M.M. Baum, Artificial photosynthesis: semiconductor photocatalytic fixation of CO<sub>2</sub> to afford higher organic compounds, *Dalton Trans.* 40 (2011) 5151–5158.
- [3] I. Ganesh, Conversion of carbon dioxide into methanol – a potential liquid fuel: Fundamental challenges and opportunities (a review), *Renew. Sust. Energ. Rev.* 31 (2014) 221–257.
- [4] T.P. Nguyen, D.M. Tuan Nguyen, D.L. Tran, H.K. Le, D.-V.-N. Vo, S.S. Lam, R.S. Varma, M. Shokouhimehr, C.C. Nguyen, Q.V. Le, MXenes: Applications in electrocatalytic, photocatalytic hydrogen evolution reaction and CO<sub>2</sub> reduction, *Molecular, Catalysis* 486 (2020) 110850.
- [5] M.A. Tekalgne, H.H. Do, A. Hasani, Q. Van Le, H.W. Jang, S.H. Ahn, S.Y. Kim, Two-dimensional materials and metal-organic frameworks for the CO<sub>2</sub> reduction reaction, *Materials Today Advances* 5 (2020) 100038.
- [6] T.P. Nguyen, D.L.T. Nguyen, V.-H. Nguyen, T.-H. Le, D.-V.-N. Vo, Q.T. Trinh, S.-R. Bae, S.Y. Chae, S.Y. Kim, Q.V. Le, Recent Advances in TiO<sub>2</sub>-Based Photocatalysts for Reduction of CO<sub>2</sub> to Fuels, *Nanomaterials* 10 (2020) 337.
- [7] A. Hasani, M. Tekalgne, Q.V. Le, H.W. Jang, S.Y. Kim, Two-dimensional materials as catalysts for solar fuels: hydrogen evolution reaction and CO<sub>2</sub> reduction, *J. Mater. Chem. A* 7 (2019) 430–454.
- [8] V.-H. Nguyen, J.C.S. Wu, Recent developments in the design of photoreactors for solar energy conversion from water splitting and CO<sub>2</sub> reduction, *Appl. Catal., A* 550 (2018) 122–141.
- [9] B.-R. Chen, V.-H. Nguyen, J.C.S. Wu, R. Martin, K. Kočí, Production of renewable fuels by the photohydrogenation of CO<sub>2</sub>: effect of the Cu species loaded onto TiO<sub>2</sub> photocatalysts, *Phys. Chem. Chem. Phys.* 18 (2016) 4942–4951.
- [10] Y.-H. Cheng, V.-H. Nguyen, H.-Y. Chan, J.C.S. Wu, W.-H. Wang, Photo-enhanced hydrogenation of CO<sub>2</sub> to mimic photosynthesis by CO co-feed in a novel twin reactor, *Appl Energy* 147 (2015) 318–324.
- [11] C.-Y. Chen, J.C.-C. Yu, V.-H. Nguyen, J.C.-S. Wu, W.-H. Wang, K. Kočí, Reactor Design for CO<sub>2</sub> Photo-Hydrogenation toward Solar Fuels under Ambient Temperature and Pressure, *Catalysts* 7 (2017) 63.
- [12] S.-H. Yu, C.-W. Chiu, Y.-T. Wu, C.-H. Liao, V.-H. Nguyen, J.C.S. Wu, Photocatalytic water splitting and hydrogenation of CO<sub>2</sub> in a novel twin photoreactor with IO<sub>3</sub><sup>-</sup>/I<sup>-</sup> shuttle redox mediator, *Appl. Catal., A* 518 (2016) 158–166.
- [13] N.-N. Vu, S. Kaliaguine, T.-O. Do, Critical Aspects and Recent Advances in Structural Engineering of Photocatalysts for Sunlight-Driven Photocatalytic Reduction of CO<sub>2</sub> into Fuels, *Adv. Funct. Mater.* 29 (2019) 1901825.
- [14] F. Zhang, Y.-H. Li, M.-Y. Qi, Z.-R. Tang, Y.-J. Xu, Boosting the activity and stability of Ag-Cu<sub>2</sub>O/ZnO nanorods for photocatalytic CO<sub>2</sub> reduction, *Appl. Catal. B* 268 (2020) 118380.
- [15] W. Dai, J. Yu, S. Luo, X. Hu, L. Yang, S. Zhang, B. Li, X. Luo, J. Zou, WS<sub>2</sub> quantum dots seeding in Bi<sub>2</sub>S<sub>3</sub> nanotubes: A novel Vis-NIR light sensitive photocatalyst with low-resistance junction interface for CO<sub>2</sub> reduction, *Chem. Eng. J.* 389 (2020) 123430.
- [16] W. Yu, D. Xu, T. Peng, Enhanced photocatalytic activity of g-C<sub>3</sub>N<sub>4</sub> for selective CO<sub>2</sub> reduction to CH<sub>3</sub>OH via facile coupling of ZnO: a direct Z-scheme mechanism, *J. Mater. Chem. A* 3 (2015) 19936–19947.
- [17] Y. Xia, Z. Tian, T. Heil, A. Meng, B. Cheng, S. Cao, J. Yu, M. Antonietti, Highly Selective CO<sub>2</sub> Capture and Its Direct Photochemical Conversion on Ordered 2D/1D Heterojunctions, *Joule* 3 (2019) 2792–2805.
- [18] H. Wang, Y. Wang, L. Guo, X. Zhang, C. Ribeiro, T. He, Solar-heating boosted catalytic reduction of CO<sub>2</sub> under full-solar spectrum, *Chinese J. Catal.* 41 (2020) 131–139.
- [19] C. Bie, B. Zhu, F. Xu, L. Zhang, J. Yu, In Situ Grown Monolayer N-Doped Graphene on CdS Hollow Spheres with Seamless Contact for Photocatalytic CO<sub>2</sub> Reduction, *Adv. Mater.* 31 (2019) 1902868.
- [20] M. Xu, A. Zada, R. Yan, H. Li, N. Sun, Y. Qu, Ti<sub>2</sub>O<sub>3</sub>/TiO<sub>2</sub> heterophase junctions with enhanced charge separation and spatially separated active sites for photocatalytic CO<sub>2</sub> reduction, *Phys. Chem. Chem. Phys.* 22 (2020) 4526–4532.
- [21] D. Li, M. Kassymova, X. Cai, S.-Q. Zang, H.-L. Jiang, Photocatalytic CO<sub>2</sub> reduction

- over metal-organic framework-based materials, *Coord. Chem. Rev.* 412 (2020) 213262.
- [22] J. Cai, F. Shen, Z. Shi, Y. Lai, J. Sun, Nanostructured TiO<sub>2</sub> for light-driven CO<sub>2</sub> conversion into solar fuels, *APL Mater.* 8 (2020) 040914.
- [23] I.I. Alkhatib, C. Garlisi, M. Pagliaro, K. Al-Ali, G. Palmisano, Metal-organic frameworks for photocatalytic CO<sub>2</sub> reduction under visible radiation: A review of strategies and applications, *Catal. Today* 340 (2020) 209–224.
- [24] M.M. Kandy, Carbon-based photocatalysts for enhanced photocatalytic reduction of CO<sub>2</sub> to solar fuels, *Sustain. Energ. Fuels* 4 (2020) 469–484.
- [25] S. Al Jitan, G. Palmisano, C. Garlisi, Synthesis and Surface Modification of TiO<sub>2</sub>-Based Photocatalysts for the Conversion of CO<sub>2</sub>, *Catalysts* 10 (2020) 227.
- [26] X. Gao, W. Yang, Reaction: Key Issues of Solar-Driven CO<sub>2</sub> Conversion to Fuel, *Chem* 6 (2020) 1041–1042.
- [27] T. Kong, J. Low, Y. Xiong, Catalyst: How Material Chemistry Enables Solar-Driven CO<sub>2</sub> Conversion, *Chem* 6 (2020) 1035–1038.
- [28] Y. Xia, J. Yu, Reaction: Rational Design of Highly Active Photocatalysts for CO<sub>2</sub> Conversion, *Chem* 6 (2020) 1039–1040.
- [29] G. Liu, N. Hoivik, K. Wang, H. Jakobsen, Engineering TiO<sub>2</sub> nanomaterials for CO<sub>2</sub> conversion/solar fuels, *Sol. Energy Mater. Sol. Cells* 105 (2012) 53–68.
- [30] E. Karamian, S. Sharifnia, On the general mechanism of photocatalytic reduction of CO<sub>2</sub>, *J. CO<sub>2</sub> Utilizat.* 16 (2016) 194–203.
- [31] H.H. Do, D.L.T. Nguyen, X.C. Nguyen, T.-H. Lee, T.P. Nguyen, Q.T. Trinh, S.H. Ahn, D.-V.N. Vo, S.Y. Kim, Q.V. Le, Recent progress in TiO<sub>2</sub>-based photocatalysts for hydrogen evolution reaction: a review, *Arab. J. Chem.* 13 (2020) 3653–3671.
- [32] M.A. Tekalgne, A. Hasani, D.Y. Heo, Q. Van Le, T.P. Nguyen, T.H. Lee, S.H. Ahn, H.W. Jang, S.Y. Kim, SnO<sub>2</sub>@WS<sub>2</sub>/p-Si Heterostructure Photocathode for Photoelectrochemical Hydrogen Production, *J. Phys. Chem. C* 124 (2020) 647–652.
- [33] A. Hasani, Q.V. Le, M. Tekalgne, M.-J. Choi, T.H. Lee, H.W. Jang, S.Y. Kim, Direct synthesis of two-dimensional MoS<sub>2</sub> on p-type Si and application to solar hydrogen production, *NPG Asia Mater.* 11 (2019) 47.
- [34] M. Tekalgne, A. Hasani, Q.V. Le, T.P. Nguyen, K.S. Choi, T.H. Lee, H.W. Jang, Z. Luo, S.Y. Kim, CdSe Quantum Dots Doped WS<sub>2</sub> Nanoflowers for Enhanced Solar Hydrogen Production, *Phys. Status Solidi A Appl. Res.* 216 (2019) 1800853.
- [35] M. Tekalgne, A. Hasani, Q. Van Le, S.Y. Kim, Transition metal dichalcogenide-based composites for hydrogen production, *Funct. Compos. Struct.* 1 (2019) 012001.
- [36] W. Guo, Q.V. Le, H.H. Do, A. Hasani, M. Tekalgne, S.-R. Bae, T.H. Lee, H.W. Jang, S.H. Ahn, S.Y. Kim, Ni<sub>3</sub>Se<sub>4</sub>@MoSe<sub>2</sub> Composites for Hydrogen Evolution Reaction, *Appl. Sci.* 9 (2019) 5035.
- [37] A. Hasani, T.P. Nguyen, M. Tekalgne, Q. Van Le, K.S. Choi, T.H. Lee, T. Jung Park, H.W. Jang, S.Y. Kim, The role of metal dopants in WS<sub>2</sub> nanoflowers in enhancing the hydrogen evolution reaction, *Appl. Catal., A* 567 (2018) 73–79.
- [38] T.P. Nguyen, Q.V. Le, S. Choi, T.H. Lee, S.-P. Hong, K.S. Choi, H.W. Jang, M.H. Lee, T.J. Park, S.Y. Kim, Surface extension of MeS<sub>2</sub> (Me = Mo or W) nanosheets by embedding MeS<sub>x</sub> for hydrogen evolution reaction, *Electrochim. Acta* 292 (2018) 136–141.
- [39] T.P. Nguyen, D.L.T. Nguyen, V.-H. Nguyen, T.-H. Lee, Q.V. Ly, D.-V.N. Vo, Q.V. Nguyen, H.S. Lee, H.W. Jang, S.Y. Kim, Q.V. Le, Facile synthesis of WS<sub>2</sub> hollow spheres and their hydrogen evolution reaction performance, *Appl. Surf. Sci.* 505 (2020) 144574.
- [40] M.A. Tekalgne, K.V. Nguyen, D.L.T. Nguyen, V.-H. Nguyen, T.P. Nguyen, D.-V.N. Vo, Q.T. Trinh, A. Hasani, H.H. Do, S.P. Lee, H.W. Jang, H.S. Lee, Q.V. Le, S.Y. Kim, Hierarchical molybdenum disulfide on carbon nanotube-reduced graphene oxide composite paper as efficient catalysts for hydrogen evolution reaction, *J. Alloys Compd.* 823 (2020) 153897.
- [41] V.-H. Nguyen, B.-S. Nguyen, C. Hu, C.C. Nguyen, D.L.T. Nguyen, M.T. Nguyen Dinh, D.-V.N. Vo, Q.T. Trinh, M. Shokouhimehr, A. Hasani, S.Y. Kim, Q.V. Le, Novel Architecture Titanium Carbide (Ti<sub>3</sub>C<sub>2</sub>T<sub>x</sub>) MXene Cocatalysts toward Photocatalytic Hydrogen Production: A Mini-Review, *Nanomaterials* 10 (2020) 602.
- [42] W. Guo, Q.V. Le, A. Hasani, T.H. Lee, H.W. Jang, Z. Luo, S.Y. Kim, MoSe<sub>2</sub>-GO/rGO Composite Catalyst for Hydrogen Evolution Reaction, *Polymers* 10 (2018) 1309.
- [43] S.S. Lam, V.-H. Nguyen, M.T. Nguyen Dinh, D.Q. Khieu, D.D. La, H.T. Nguyen, D.-V.N. Vo, C. Xia, R.S. Varma, M. Shokouhimehr, C.C. Nguyen, Q.V. Le, W. Peng, Mainstream avenues for boosting graphitic carbon nitride efficiency: towards enhanced solar light-driven photocatalytic hydrogen production and environmental remediation, *J. Mater. Chem. A* 8 (2020) 10571–10603.
- [44] T. Inoue, A. Fujishima, S. Konishi, K. Honda, Photoelectrocatalytic reduction of carbon dioxide in aqueous suspensions of semiconductor powders, *Nature* 277 (1979) 637–638.
- [45] P.D. Tran, L.H. Wong, J. Barber, J.S.C. Loo, Recent advances in hybrid photocatalysts for solar fuel production, *Energy Environ. Sci.* 5 (2012) 5902–5918.
- [46] K.R. Thampi, J. Kiwi, M. Grätzel, Methanation and photo-methanation of carbon dioxide at room temperature and atmospheric pressure, *Nature* 327 (1987) 506–508.
- [47] C.-C. Lo, C.-H. Hung, C.-S. Yuan, J.-F. Wu, Photoreduction of carbon dioxide with H<sub>2</sub> and H<sub>2</sub>O over TiO<sub>2</sub> and ZrO<sub>2</sub> in a circulated photocatalytic reactor, *Sol. Energy Mater. Sol. Cells* 91 (2007) 1765–1774.
- [48] Y. Kohno, H. Hayashi, S. Takenaka, T. Tanaka, T. Funabiki, S. Yoshida, Photo-enhanced reduction of carbon dioxide with hydrogen over Rh/TiO<sub>2</sub>, *J. Photochem. Photobiol. A* 126 (1999) 117–123.
- [49] M. Li, P. Li, K. Chang, T. Wang, L. Liu, Q. Kang, S. Ouyang, J. Ye, Highly efficient and stable photocatalytic reduction of CO<sub>2</sub> to CH<sub>4</sub> over Ru loaded NaTaO<sub>3</sub>, *Chem. Commun.* 51 (2015) 7645–7648.
- [50] F. Sastre, A.V. Puga, L. Liu, A. Corma, H. García, Complete Photocatalytic Reduction of CO<sub>2</sub> to Methane by H<sub>2</sub> under Solar Light Irradiation, *J. Am. Chem. Soc.* 136 (2014) 6798–6801.
- [51] K. Teramura, H. Tsuneko, T. Shishido, T. Tanaka, Effect of H<sub>2</sub> gas as a reductant on photoreduction of CO<sub>2</sub> over a Ga<sub>2</sub>O<sub>3</sub> photocatalyst, *Chem. Phys. Lett.* 467 (2008) 191–194.
- [52] M. Tahir, B. Tahir, N.A.S. Amin, Z.Y. Zakaria, Photo-induced reduction of CO<sub>2</sub> to CO with hydrogen over plasmonic Ag-NPs/TiO<sub>2</sub> NWs core/shell hetero-junction under UV and visible light, *J. CO<sub>2</sub> Util.* 18 (2017) 250–260.
- [53] M. Tahir, N.A.S. Amin, Photo-induced CO<sub>2</sub> reduction by hydrogen for selective CO evolution in a dynamic monolith photoreactor loaded with Ag-modified TiO<sub>2</sub> nanocatalyst, *Int. J. Hydrogen Energy* 42 (2017) 15507–15522.
- [54] B. Tahir, M. Tahir, N.A.S. Amin, Photocatalytic CO<sub>2</sub> conversion over Au/TiO<sub>2</sub> nanostructures for dynamic production of clean fuels in a monolith photoreactor, *Clean Technol. Environ. Policy* 18 (2016) 2147–2160.
- [55] Y. Kohno, H. Ishikawa, T. Tanaka, T. Funabiki, S. Yoshida, Photoreduction of carbon dioxide by hydrogen over magnesium oxide, *Phys. Chem. Chem. Phys.* 3 (2001) 1108–1113.
- [56] K. Teramura, T. Tanaka, H. Ishikawa, Y. Kohno, T. Funabiki, Photocatalytic Reduction of CO<sub>2</sub> to CO in the Presence of H<sub>2</sub> or CH<sub>4</sub> as a Reductant over MgO, *J. Phys. Chem. B* 108 (2004) 346–354.
- [57] T. Tanaka, Y. Kohno, S. Yoshida, Photoreduction of carbon dioxide by hydrogen and methane, *Res. Chem. Intermediat.* 26 (2000) 93–101.
- [58] H. Tsuneko, K. Teramura, T. Shishido, T. Tanaka, Adsorbed Species of CO<sub>2</sub> and H<sub>2</sub> on Ga<sub>2</sub>O<sub>3</sub> for the Photocatalytic Reduction of CO<sub>2</sub>, *J. Phys. Chem. C* 114 (2010) 8892–8898.
- [59] K. Teramura, T. Tanaka, Photocatalytic Reduction of CO<sub>2</sub> Using H<sub>2</sub> as Reductant over Solid Base Photocatalysts, *Advances in CO<sub>2</sub> Conversion and Utilization*, Am. Chem. Soc. (2010) 15–24.
- [60] N. Ahmed, Y. Shibata, T. Taniguchi, Y. Izumi, Photocatalytic conversion of carbon dioxide into methanol using zinc-copper-M(III) (M = aluminum, gallium) layered double hydroxides, *J. Catal.* 279 (2011) 123–135.
- [61] N. Ahmed, M. Morikawa, Y. Izumi, Photocatalytic conversion of carbon dioxide into methanol using optimized layered double hydroxide catalysts, *Catal. Today* 185 (2012) 263–269.
- [62] H. Robatjazi, H. Zhao, D.F. Swearer, N.J. Hogan, L. Zhou, A. Alabastri, M.J. McClain, P. Nordlander, N.J. Halas, Plasmon-induced selective carbon dioxide conversion on earth-abundant aluminum-cuprous oxide antenna-reactor nanoparticles, *Nat. Commun.* 8 (2017) 27.
- [63] B. Alotaibi, X. Kong, S. Vanka, S.Y. Woo, A. Pofelski, F. Oudjedi, S. Fan, M.G. Kibria, G.A. Botton, W. Ji, H. Guo, Z. Mi, Photochemical Carbon Dioxide Reduction on Mg-Doped Ga(In) Nanowire Arrays under Visible Light Irradiation, *ACS Energy Lett.* 1 (2016) 246–252.
- [64] Q. Kang, T. Wang, P. Li, L. Liu, K. Chang, M. Li, J. Ye, Photocatalytic Reduction of Carbon Dioxide by Hydrous Hydrazine over Au-Cu Alloy Nanoparticles Supported on SrTiO<sub>3</sub>/TiO<sub>2</sub> Coaxial Nanotube Arrays, *Angew. Chem. Int. Ed.* 54 (2015) 841–845.
- [65] S. Gao, B. Gu, X. Jiao, Y. Sun, X. Zu, F. Yang, W. Zhu, C. Wang, Z. Feng, B. Ye, Y. Xie, Highly Efficient and Exceptionally Durable CO<sub>2</sub> Photoreduction to Methanol over Freestanding Defective Single-Unit-Cell Bismuth Vanadate Layers, *J. Am. Chem. Soc.* 139 (2017) 3438–3445.
- [66] G. Guan, T. Kida, A. Yoshida, Reduction of carbon dioxide with water under concentrated sunlight using photocatalyst combined with Fe-based catalyst, *Appl. Catal. B* 41 (2003) 387–396.
- [67] S. Bai, C. Gao, J. Low, Y. Xiong, Crystal phase engineering on photocatalytic materials for energy and environmental applications, *Nano Res.* 12 (2019) 2031–2054.
- [68] H. Shen, T. Peppel, J. Stunk, Z. Sun, Photocatalytic Reduction of CO<sub>2</sub> by Metal-Free-Based Materials: Recent Advances and Future Perspective, *Solar RRL*. doi:10.1002/solr.201900546.
- [69] J. Xiong, P. Song, J. Di, H. Li, Ultrathin structured photocatalysts: A versatile platform for CO<sub>2</sub> reduction, *Appl. Catal. B* 256 (2019) 117788.
- [70] X. Li, J. Yu, M. Jaroniec, X. Chen, Cocatalysts for Selective Photoreduction of CO<sub>2</sub> into Solar Fuels, *Chem. Rev.* 119 (2019) 3962–4179.
- [71] L. Ye, Y. Deng, L. Wang, H. Xie, F. Su, Bismuth-Based Photocatalysts for Solar Photocatalytic Carbon Dioxide Conversion, *ChemSusChem* 12 (2019) 3671–3701.
- [72] J. Fu, K. Jiang, X. Qiu, J. Yu, M. Liu, Product selectivity of photocatalytic CO<sub>2</sub> reduction reactions, *Mater. Today* 32 (2020) 222–243.
- [73] S. Chen, Y. Qi, C. Li, K. Domen, F. Zhang, Surface Strategies for Particulate Photocatalysts toward Artificial Photosynthesis, *Joule* 2 (2018) 2260–2288.
- [74] G. Chen, G.I.N. Waterhouse, R. Shi, J. Zhao, Z. Li, L.-Z. Wu, C.-H. Tung, T. Zhang, From Solar Energy to Fuels: Recent Advances in Light-Driven C-I Chemistry, *Angew. Chem. Int. Ed.* 58 (2019) 17528–17551.
- [75] Z. Chen, H. Zhang, P. Guo, J. Zhang, G. Tira, Y.J. Kim, Y.A. Wu, Y. Liu, J. Wen, T. Rajh, J. Niklas, O.G. Poluektov, P.D. Laible, E.A. Rozhkova, Semi-artificial Photosynthetic CO<sub>2</sub> Reduction through Purple Membrane Re-engineering with Semiconductor, *J. Am. Chem. Soc.* 141 (2019) 11811–11815.
- [76] G. Zhang, Z.-A. Lan, L. Lin, S. Lin, X. Wang, Overall water splitting by Pt/g-C<sub>3</sub>N<sub>4</sub> photocatalysts without using sacrificial agents, *Chem. Sci.* 7 (2016) 3062–3066.
- [77] Q. Wang, K. Wang, L. Zhang, H. Wang, W. Wang, Photocatalytic reduction of CO<sub>2</sub> to methane over PtO<sub>x</sub>-loaded ultrathin Bi<sub>2</sub>WO<sub>6</sub> nanosheets, *Appl. Surf. Sci.* 470 (2019) 832–839.
- [78] Y. Izumi, Recent advances in the photocatalytic conversion of carbon dioxide to fuels with water and/or hydrogen using solar energy and beyond, *Coord. Chem. Rev.* 257 (2013) 171–186.
- [79] M. Tahir, B. Tahir, N.A.S. Amin, Gold-nanoparticle-modified TiO<sub>2</sub> nanowires for plasmon-enhanced photocatalytic CO<sub>2</sub> reduction with H<sub>2</sub> under visible light

- irradiation, *Appl. Surf. Sci.* 356 (2015) 1289–1299.
- [80] J. Ye, C. Liu, D. Mei, Q. Ge, Active Oxygen Vacancy Site for Methanol Synthesis from CO<sub>2</sub> Hydrogenation on In<sub>2</sub>O<sub>3</sub>(110): A DFT Study, *ACS Catal.* 3 (2013) 1296–1306.
- [81] K.K. Ghuman, L.B. Hoch, P. Szymanski, J.Y.Y. Loh, N.P. Kherani, M.A. El-Sayed, G.A. Ozin, C.V. Singh, Photoexcited Surface Frustrated Lewis Pairs for Heterogeneous Photocatalytic CO<sub>2</sub> Reduction, *J. Am. Chem. Soc.* 138 (2016) 1206–1214.
- [82] K.K. Ghuman, T.E. Wood, L.B. Hoch, C.A. Mims, G.A. Ozin, C.V. Singh, Illuminating CO<sub>2</sub> reduction on frustrated Lewis pair surfaces: investigating the role of surface hydroxides and oxygen vacancies on nanocrystalline In<sub>2</sub>O<sub>3-x</sub>(OH)<sub>y</sub>, *Phys. Chem. Chem. Phys.* 17 (2015) 14623–14635.
- [83] L. He, T.E. Wood, B. Wu, Y. Dong, L.B. Hoch, L.M. Reyes, D. Wang, C. Kübel, C. Qian, J. Jia, K. Liao, P.G. O'Brien, A. Sandhel, J.Y.Y. Loh, P. Szymanski, N.P. Kherani, T.C. Sum, C.A. Mims, G.A. Ozin, Spatial Separation of Charge Carriers in In<sub>2</sub>O<sub>3-x</sub>(OH)<sub>y</sub> Nanocrystal Superstructures for Enhanced Gas-Phase Photocatalytic Activity, *ACS Nano* 10 (2016) 5578–5586.
- [84] H. Wang, J. Jia, L. Wang, K. Butler, R. Song, G. Casillas, L. He, N.P. Kherani, D.D. Perovic, L. Jing, A. Walsh, R. Dittmeyer, G.A. Ozin, Heterostructure Engineering of a Reverse Water Gas Shift Photocatalyst, *Adv. Sci.* 6 (2019) 1902170.
- [85] S.S. Kim, H.H. Lee, S.C. Hong, The effect of the morphological characteristics of TiO<sub>2</sub> supports on the reverse water–gas shift reaction over Pt/TiO<sub>2</sub> catalysts, *Appl. Catal. B* 119–120 (2012) 100–108.
- [86] B. Lu, F. Quan, Z. Sun, F. Jia, L. Zhang, Photothermal reverse-water-gas-shift over Au/CeO<sub>2</sub> with high yield and selectivity in CO<sub>2</sub> conversion, *Catal. Commun.* 129 (2019) 105724.
- [87] N. Ishito, K. Hara, K. Nakajima, A. Fukuoka, Selective synthesis of carbon monoxide via formates in reverse water–gas shift reaction over alumina-supported gold catalyst, *J. Energy Chem.* 25 (2016) 306–310.
- [88] S. Mukherjee, F. Libisch, N. Lorge, O. Neumann, L.V. Brown, J. Cheng, J.B. Lassiter, E.A. Carter, P. Nordlander, N.J. Halas, Hot Electrons Do the Impossible: Plasmon-Induced Dissociation of H<sub>2</sub> on Au, *Nano Lett.* 13 (2013) 240–247.
- [89] X. Zhang, X. Li, D. Zhang, N.Q. Su, W. Yang, H.O. Everitt, J. Liu, Product selectivity in plasmonic photocatalysis for carbon dioxide hydrogenation, *Nat. Commun.* 8 (2017) 14542.
- [90] A.A. Upadhye, I. Ro, X. Zeng, H.J. Kim, I. Tejedor, M.A. Anderson, J.A. Dumesic, G.W. Huber, Plasmon-enhanced reverse water gas shift reaction over oxide supported Au catalysts, *Catal. Sci. Technol.* 5 (2015) 2590–2601.
- [91] J. Jia, P.G. O'Brien, L. He, Q. Qiao, T. Fei, L.M. Reyes, T.E. Burrow, Y. Dong, K. Liao, M. Varela, S.J. Pennycook, M. Hmadeh, A.S. Helmy, N.P. Kherani, D.D. Perovic, G.A. Ozin, Visible and Near-Infrared Photothermal Catalyzed Hydrogenation of Gaseous CO<sub>2</sub> over Nanostructured Pd@Nb<sub>2</sub>O<sub>5</sub>, *Adv. Sci.* 3 (2016) 1600189.
- [92] Y.F. Li, N. Soheilnia, M. Greiner, U. Ulmer, T. Wood, A.A. Jelle, Y. Dong, A.P. Yin Wong, J. Jia, G.A. Ozin, Pd@H<sub>2</sub>WO<sub>3-x</sub> Nanowires Efficiently Catalyze the CO<sub>2</sub> Heterogeneous Reduction Reaction with a Pronounced Light Effect, *ACS Appl. Mater. Interfaces* 11 (2019) 5610–5615.
- [93] Y.F. Li, W. Lu, K. Chen, P. Duchesne, A. Jelle, M. Xia, T.E. Wood, U. Ulmer, G.A. Ozin, Cu Atoms on Nanowire Pd/H<sub>2</sub>WO<sub>3-x</sub> Bronzes Enhance the Solar Reverse Water Gas Shift Reaction, *J. Am. Chem. Soc.* 141 (2019) 14991–14996.
- [94] M.D. Porosoff, B. Yan, J.G. Chen, Catalytic reduction of CO<sub>2</sub> by H<sub>2</sub> for synthesis of CO, methanol and hydrocarbons: challenges and opportunities, *Energy Environ. Sci.* 9 (2016) 62–73.
- [95] L. Wang, M. Ghoussoub, H. Wang, Y. Shao, W. Sun, A.A. Tountas, T.E. Wood, H. Li, J.Y.Y. Loh, Y. Dong, M. Xia, Y. Li, S. Wang, J. Jia, C. Qiu, C. Qian, N.P. Kherani, L. He, X. Zhang, G.A. Ozin, Photocatalytic Hydrogenation of Carbon Dioxide with High Selectivity to Methanol at Atmospheric Pressure, *Joule* 2 (2018) 1369–1381.
- [96] G. Centi, E.A. Quadrelli, S. Perathoner, Catalysis for CO<sub>2</sub> conversion: a key technology for rapid introduction of renewable energy in the value chain of chemical industries, *Energy Environ. Sci.* 6 (2013) 1711–1731.
- [97] M. Tahir, B. Tahir, N.A.S. Amin, A. Muhammad, Photocatalytic CO<sub>2</sub> methanation over NiO/In<sub>2</sub>O<sub>3</sub> promoted TiO<sub>2</sub> nanocatalysts using H<sub>2</sub>O and/or H<sub>2</sub> reductants, *Energy Convers. Manage.* 119 (2016) 368–378.
- [98] X. Meng, T. Wang, L. Liu, S. Ouyang, P. Li, H. Hu, T. Kako, H. Iwai, A. Tanaka, J. Ye, Photothermal Conversion of CO<sub>2</sub> into CH<sub>4</sub> with H<sub>2</sub> over Group VIII Nanocatalysts: An Alternative Approach for Solar Fuel Production, *Angew. Chem. Int. Ed.* 53 (2014) 11478–11482.
- [99] W. Wang, S. Wang, X. Ma, J. Gong, Recent advances in catalytic hydrogenation of carbon dioxide, *Chem. Soc. Rev.* 40 (2011) 3703–3727.
- [100] Y. Chen, J. Long, Z. Li, Efficient Photothermal CO<sub>2</sub> Methanation over RuO<sub>2</sub>/SrTiO<sub>3</sub>, *Trends Chem.* 1 (2019) 459–460.
- [101] D. Mateo, J. Albero, H. García, Photoassisted methanation using Cu<sub>2</sub>O nanoparticles supported on graphene as a photocatalyst, *Energy Environ. Sci.* 10 (2017) 2392–2400.
- [102] D. Mateo, J. Albero, H. García, Titanium-Perovskite-Supported RuO<sub>2</sub> Nanoparticles for Photocatalytic CO<sub>2</sub> Methanation, *Joule* 3 (2019) 1949–1962.
- [103] J. Ren, S. Ouyang, H. Xu, X. Meng, T. Wang, D. Wang, J. Ye, Targeting Activation of CO<sub>2</sub> and H<sub>2</sub> over Ru-Loaded Ultrathin Layered Double Hydroxides to Achieve Efficient Photothermal CO<sub>2</sub> Methanation in Flow-Type System, *Adv. Energy Mater.* 7 (2017) 1601657.
- [104] D. Mateo, J. Albero, H. García, Graphene supported NiO/Ni nanoparticles as efficient photocatalyst for gas phase CO<sub>2</sub> reduction with hydrogen, *Appl. Catal. B* 224 (2018) 563–571.
- [105] C. Wang, S. Fang, S. Xie, Y. Zheng, Y.H. Hu, Thermo-photo catalytic CO<sub>2</sub> hydrogenation over Ru/TiO<sub>2</sub>, *J. Mater. Chem. A* (2020).
- [106] J. Barrio, D. Mateo, J. Albero, H. García, M. Shalom, A Heterogeneous Carbon Nitride-Nickel Photocatalyst for Efficient Low-Temperature CO<sub>2</sub> Methanation, *Adv. Energy Mater.* 9 (2019) 1902738.
- [107] B. Tahir, M. Tahir, M.A. Che Yunus, A.R. Mohamed, M. Siraj, A. Fatehmulla, 2D/2D Mt/m-CN composite with enriched interface charge transfer for boosting photocatalytic CO<sub>2</sub> hydrogenation by H<sub>2</sub> to CH<sub>4</sub> under visible light, *Appl. Surf. Sci.* 520 (2020) 146296.
- [108] M. Tahir, B. Tahir, Constructing a Stable 2D/2D Heterojunction of Oxygen-Cluster-Modified Ti<sub>3</sub>AlC<sub>2</sub> MAX Cocatalyst with Proton-Rich C<sub>3</sub>N<sub>4</sub> for Highly Efficient Photocatalytic CO<sub>2</sub> Methanation, *Ind. Eng. Chem. Res.* 59 (2020) 9841–9857.
- [109] Y. Li, J. Hao, H. Song, F. Zhang, X. Bai, X. Meng, H. Zhang, S. Wang, Y. Hu, J. Ye, Selective light absorber-assisted single nickel atom catalysts for ambient sunlight-driven CO<sub>2</sub> methanation, *Nat. Commun.* 10 (2019) 2359.
- [110] R. Zhang, Z. Huang, C. Li, Y. Zuo, Y. Zhou, Monolithic g-C<sub>3</sub>N<sub>4</sub>/reduced graphene oxide aerogel with in situ embedding of Pd nanoparticles for hydrogenation of CO<sub>2</sub> to CH<sub>4</sub>, *Appl. Surf. Sci.* 475 (2019) 953–960.
- [111] N. Karachi, M. Hosseini, Z. Parsaee, R. Razavi, Novel high performance reduced graphene oxide based nanocatalyst decorated with Rh<sub>2</sub>O<sub>3</sub>/Rh-NPs for CO<sub>2</sub> photoreduction, *J. Photochem. Photobiol. A* 364 (2018) 344–354.
- [112] M. Xu, X. Hu, S. Wang, J. Yu, D. Zhu, J. Wang, Photothermal effect promoting CO<sub>2</sub> conversion over composite photocatalyst with high graphene content, *J. Catal.* 377 (2019) 652–661.
- [113] F. Hu, S. Tong, K. Lu, C.-M. Chen, F.-Y. Su, J. Zhou, Z.-H. Lu, X. Wang, G. Feng, R. Zhang, Reduced graphene oxide supported Ni-Ce catalysts for CO<sub>2</sub> methanation: The support and ceria promotion effects, *J. CO<sub>2</sub> Utilizat.* 34 (2019) 676–687.
- [114] A. Primo, J. He, B. Jurca, B. Cojocaru, C. Bucur, V.I. Parvulescu, H. Garcia, CO<sub>2</sub> methanation catalyzed by oriented MoS<sub>2</sub> nanoplatelets supported on few layers graphene, *Appl. Catal. B* 245 (2019) 351–359.
- [115] I. Sreedhar, Y. Varun, S.A. Singh, A. Venugopal, B.M. Reddy, Developmental trends in CO<sub>2</sub> methanation using various catalysts, *Catal. Sci. Technol.* 9 (2019) 4478–4504.
- [116] S. Verma, B. Kim, H.-R.M. Jhong, S. Ma, P.J.A. Kenis, A Gross-Margin Model for Defining Technoeconomic Benchmarks in the Electroreduction of CO<sub>2</sub>, *ChemSusChem* 9 (2016) 1972–1979.
- [117] K. Jiang, R.B. Sandberg, A.J. Akey, X. Liu, D.C. Bell, J.K. Nørskov, K. Chan, H. Wang, Metal ion cycling of Cu foil for selective C-C coupling in electrochemical CO<sub>2</sub> reduction, *Nat. Catal.* 1 (2018) 111–119.
- [118] J. Albero, Y. Peng, H. García, Photocatalytic CO<sub>2</sub> Reduction to C<sub>2+</sub> Products, *ACS Catal.* 10 (2020) 5734–5749.
- [119] A.J. Garza, A.T. Bell, M. Head-Gordon, Mechanism of CO<sub>2</sub> Reduction at Copper Surfaces: Pathways to C<sub>2</sub> Products, *ACS Catal.* 8 (2018) 1490–1499.
- [120] X. Liu, J. Xiao, H. Peng, X. Hong, K. Chan, J.K. Nørskov, Understanding trends in electrochemical carbon dioxide reduction rates, *Nat. Commun.* 8 (2017) 15438.
- [121] G. Chen, R. Gao, Y. Zhao, Z. Li, G.I.N. Waterhouse, R. Shi, J. Zhao, M. Zhang, L. Shang, G. Sheng, X. Zhang, X. Wen, L.-Z. Wu, C.-H. Tung, T. Zhang, Alumina-Supported CoFe Alloy Catalysts Derived from Layered-Double-Hydroxide Nanosheets for Efficient Photothermal CO<sub>2</sub> Hydrogenation to Hydrocarbons, *Adv. Mater.* 30 (2018) 1704663.
- [122] L. Liu, A.V. Puga, J. Coreá, P. Concepción, V. Pérez-Dieste, H. García, A. Corma, Sunlight-assisted hydrogenation of CO<sub>2</sub> into ethanol and C<sub>2+</sub> hydrocarbons by sodium-promoted Co@C nanocomposites, *Appl. Catal. B* 235 (2018) 186–196.
- [123] W. Wang, X. Jiang, X. Wang, C. Song, Fe-Cu Bimetallic Catalysts for Selective CO<sub>2</sub> Hydrogenation to Olefin-Rich C<sub>2+</sub> Hydrocarbons, *Ind. Eng. Chem. Res.* 57 (2018) 4535–4542.
- [124] M. Fujiwara, H. Sakurai, K. Shiokawa, Y. Iizuka, Synthesis of C<sub>2+</sub> hydrocarbons by CO<sub>2</sub> hydrogenation over the composite catalyst of Cu–Zn–Al oxide and HB zeolite using two-stage reactor system under low pressure, *Catal. Today* 242 (2015) 255–260.
- [125] Y. Mi, X. Peng, X. Liu, J. Luo, Selective Formation of C<sub>2</sub> Products from Electrochemical CO<sub>2</sub> Reduction over Cu<sub>1.8</sub>Se Nanowires, *ACS Appl. Energy Mater.* 1 (2018) 5119–5123.
- [126] D.R. Kauffman, D. Alfonso, Directing CO<sub>2</sub> conversion with copper nanoneedles, *Nat. Catal.* 1 (2018) 99–100.
- [127] L. Fan, C. Xia, F. Yang, J. Wang, H. Wang, Y. Lu, Strategies in catalysts and electrolyzer design for electrochemical CO<sub>2</sub> reduction toward C<sub>2+</sub> products, *Sci. Adv.* 6 (2020) eaay3111.
- [128] Z. Gu, H. Shen, L. Shang, X. Lv, L. Qian, G. Zheng, Nanostructured Copper-Based Electrocatalysts for CO<sub>2</sub> Reduction, *Small Methods* 2 (2018) 1800121.
- [129] E.T. Kho, T.H. Tan, E. Lovell, R.J. Wong, J. Scott, R. Amal, A review on photo-thermal catalytic conversion of carbon dioxide, *Green Energy Environ.* 2 (2017) 204–217.
- [130] Z. Xiong, Z. Lei, B. Gong, X. Chen, Y. Zhao, J. Zhang, C. Zheng, J.C.S. Wu, A novel reaction mode using H<sub>2</sub> produced from solid-liquid reaction to promote CO<sub>2</sub> reduction through solid-gas reaction, *Catal. Commun.* 89 (2017) 4–8.
- [131] R. Abe, K. Sayama, K. Domen, H. Arakawa, A new type of water splitting system composed of two different TiO<sub>2</sub> photocatalysts (anatase, rutile) and a IO<sub>3</sub><sup>-</sup>/I<sup>-</sup> shuttle redox mediator, *Chem. Phys. Lett.* 344 (2001) 339–344.
- [132] W.-H. Lee, C.-H. Liao, M.-F. Tsai, C.-W. Huang, J.C.S. Wu, A novel twin reactor for CO<sub>2</sub> photoreduction to mimic artificial photosynthesis, *Appl. Catal. B* 132–133 (2013) 445–451.
- [133] Z. Xiong, C.-C. Kuang, K.-Y. Lin, Z. Lei, X. Chen, B. Gong, J. Yang, Y. Zhao, J. Zhang, B. Xia, J.C.S. Wu, Enhanced CO<sub>2</sub> photocatalytic reduction through simultaneously accelerated H<sub>2</sub> evolution and CO<sub>2</sub> hydrogenation in a twin photo-reactor, *J. CO<sub>2</sub> Utilizat.* 24 (2018) 500–508.
- [134] S. Li, L. Yang, O. Ola, M. Maroto-Valer, X. Du, Y. Yang, Photocatalytic reduction of

- CO<sub>2</sub> by CO co-feed combined with photocatalytic water splitting in a novel twin reactor, *Energy Convers. Manage.* 116 (2016) 184–193.
- [135] F. Chu, S. Li, H. Chen, L. Yang, O. Ola, M. Maroto-Valer, X. Du, Y. Yang, Modeling photocatalytic conversion of carbon dioxide in bubbling twin reactor, *Energy Convers. Manage.* 149 (2017) 514–525.
- [136] H. Zhou, J. Guo, P. Li, T. Fan, D. Zhang, J. Ye, Leaf-architected 3D Hierarchical Artificial Photosynthetic System of Perovskite Titanates Towards CO<sub>2</sub> Photoreduction Into Hydrocarbon Fuels, *Sci. Rep.* 3 (2013) 1667.
- [137] Y. Sohn, W. Huang, F. Taghipour, Recent progress and perspectives in the photocatalytic CO<sub>2</sub> reduction of Ti-oxide-based nanomaterials, *Appl. Surf. Sci.* 396 (2017) 1696–1711.
- [138] C.-Y. Lee, J. Zou, J. Bullock, G.G. Wallace, Emerging approach in semiconductor photocatalysis: Towards 3D architectures for efficient solar fuels generation in semi-artificial photosynthetic systems, *J. Photochem. Photobiol. C: Photochem. Rev.* 39 (2019) 142–160.
- [139] E.M. Nichols, J.J. Gallagher, C. Liu, Y. Su, J. Resasco, Y. Yu, Y. Sun, P. Yang, M.C.Y. Chang, C.J. Chang, Hybrid bioinorganic approach to solar-to-chemical conversion, *Proc. Natl. Acad. Sci. U. S. A.* 112 (2015) 11461–11466.
- [140] J.P. Torella, C.J. Gagliardi, J.S. Chen, D.K. Bediako, B. Colón, J.C. Way, P.A. Silver, D.G. Nocera, Efficient solar-to-fuels production from a hybrid microbial–water-splitting catalyst system, *Proc. Natl. Acad. Sci. U. S. A.* 112 (2015) 2337–2342.
- [141] C. Liu, B.C. Colón, M. Ziesack, P.A. Silver, D.G. Nocera, Water splitting–biosynthetic system with CO<sub>2</sub> reduction efficiencies exceeding photosynthesis, *Science* 352 (2016) 1210–1213.
- [142] H. Li, P.H. Opgenorth, D.G. Wernick, S. Rogers, T.-Y. Wu, W. Higashide, P. Malati, Y.-X. Huo, K.M. Cho, J.C. Liao, Integrated Electromicrobial Conversion of CO<sub>2</sub> to Higher Alcohols, *Science* 335 (2012) 1596–1596.